

BREEZE - Bioinspired Ray for Extreme Environments and Zonal Exploration

NIAC Phase I Final Report

Principle Investigator: **Javid Bayandor**

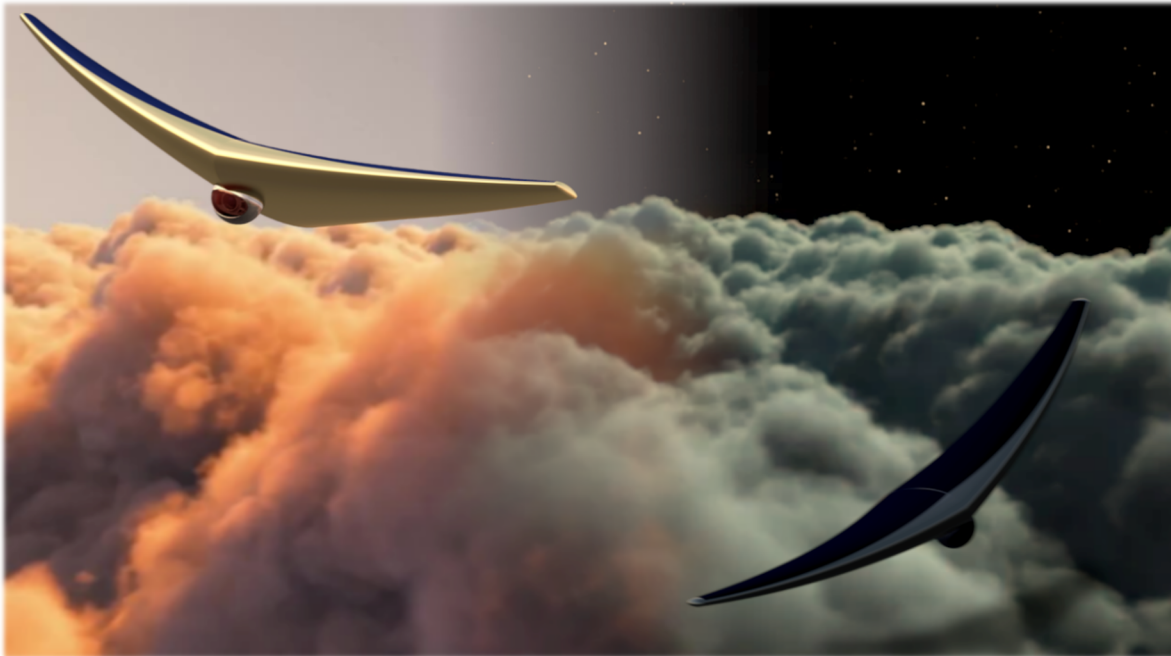
*CR*ashworthiness for *A*erospace *S*tructures and *H*ybrids (*CRASH*) Lab
Department of Mechanical and Aerospace Engineering
University at Buffalo (UB) – The State University of New York

CO-Investigator: **Jamshid Samareh**, Vehicle Analysis Branch, NASA Langley Research Center

Postdoctoral Associate: **Alexander Matta**, *CRASH* Lab

Graduate Researcher: **Munjal Shah**, CREST Lab

Undergraduate Researchers: **Tyler Chau, Lia Knoer, Justin Page, Matthew Thornton**, *CRASH* Lab



Contents

1. Executive Summary	3
2. Concept Overview.....	4
3. Mission overview.....	7
3.1. Earth to Venus Transfer and EDI.....	7
3.2. Operating Conditions and Flight Path.....	8
3.3. Instrumentation and Science Objectives	10
4. Bioinspired Propulsion Analysis	11
4.1. Numerical Methods	12
4.2. Kinematic Parameters.....	13
4.3. CFD Results and Discussion	15
5. Flight Dynamics and Stability.....	23
5.1. Modeling Methods.....	23
5.2. Baseline Results	25
5.3. Parametric Study Results	29
6. Structure Analysis and Mass Estimates	31
6.1. Finite Element Model.....	31
6.2. Structural Parametric Studies.....	32
6.3. Structural Scaling Effects.....	34
6.4. Mass Breakdown of BREEZE	36
7. Broader Impact.....	37
8. Future work.....	37
9. Conclusion	38
10. References	39

1. Executive Summary

The Bio-inspired Ray for Extreme Environments and Zonal Exploration (BREEZE) combines inflatable structures with bioinspired propulsion to create a versatile flyer for exploration of the Venusian atmosphere. BREEZE will navigate the atmosphere at altitudes between 50 to 60 km, while riding zonal winds to circumnavigate the planet every 4 to 6 days. BREEZE's unique navigation capabilities and primary scientific payload will enable dispersed sample collection for atmospheric and geographic studies. These studies include tracking weather patterns, determining atmospheric constituents, mapping the Venusian magnetic field, and creating detailed surface scans. The science enabled by BREEZE makes it the ideal approach for the Venus Climate Mission presented in the 2013-2022 Decadal Survey.

To achieve mission objectives, BREEZE merges many aspects of previously proposed Venus flyers into a unique concept. Unlike fixed-wing flyers, the inflatable nature of BREEZE enables low-risk traversal and sample collection on the night side of Venus. BREEZE's bioinspired propulsion and buoyancy control via volume reduction provides 3-D navigation capability, unlike balloon concepts whose flight paths are determined by wind direction.

Phase I study activities included:

1. Defining and developing a conceptual mission to Venus that would utilize BREEZE
2. Determining the thrust capabilities of BREEZE's bioinspired propulsion
3. Analyzing the stability and flight dynamics of BREEZE
4. Analyzing the unique inflatable structure of BREEZE and conducting mass estimations

Key results of the Phase I study include:

1. BREEZE's bioinspired propulsion can generate net thrust at speeds of 5 m/s allowing it to make headway against Venus' meridional winds.
2. BREEZE's relative angle of attack, flapping amplitude, and Strouhal number could be tuned during flight to adjust thrust production.
3. BREEZE is stable during flight thanks to its large moment of inertia and its buoyant structure paired with a low center of gravity.
4. From a structural standpoint, BREEZE scales ideally between different size flyers. This increases its versatility and makes it suitable as a secondary payload or in a small multi-flyer mission.
5. Initial estimates indicate that BREEZE would have 18% of its mass or more available for scientific instrumentation.

2. Concept Overview

BREEZE is a coupled inflatable structures with bioinspired propulsion that creates a highly efficient flyer for exploration of the Venusian atmosphere. Other missions proposed to investigate Venus' atmosphere include atmospheric balloons and low weight lift based solar-powered flyers. Balloons have a limited life span as the meridional winds continuously push them toward the polar vortices where they can no longer operate. On the other hand, lift based solar powered flyers are able to resist the meridional winds, but cannot fly on the night-side of the planet because the continual power draw required to remain aloft. BREEZE is a hybrid concept that combines the strengths of both atmospheric flyers, while simultaneously overcoming their individual limitations. Instead of fighting against the high-speed winds in the upper atmosphere of Venus, BREEZE coasts with the wind, allowing the vehicle to be propelled around the planet. Unlike other proposed Venus flyers, the current concept is a tension based system, allowing for the removal of most rigid support structures other than those needed for the payload and cross-sectional support. The internal tensioning system is inspired by the wing-warping design of the original Wright flyer, but BREEZE takes wing warping to a new level by using it to achieve biomimetic locomotion. A network of tensioning cables will be used to actuate BREEZE's wing like pectoral fins. This will provide flapping flight for thrust, control, stability, and additional lift.

The use of flapping propulsion instead of propellers has several advantages over traditional propelled craft. With BREEZE, no external actuation mechanisms are necessary, mitigating the concerns of corrosion or heat damage. By using bioinspired design and kinematics, the craft has a much higher degree of control than existing balloon concepts, without the need for external control surfaces required in fixed-wing aircraft. As opposed to eventually being forced into stagnation at one of the poles, the vehicle would be able to generate enough thrust to overcome the low speed meridional winds, giving much greater access to various latitudes of Venus. Additionally, the tension based system allows most of the rigid support structures to be removed, not otherwise possible with a propeller design. This will enable the vehicle to be highly compact and housed in smaller entry modules (Fig. 1).

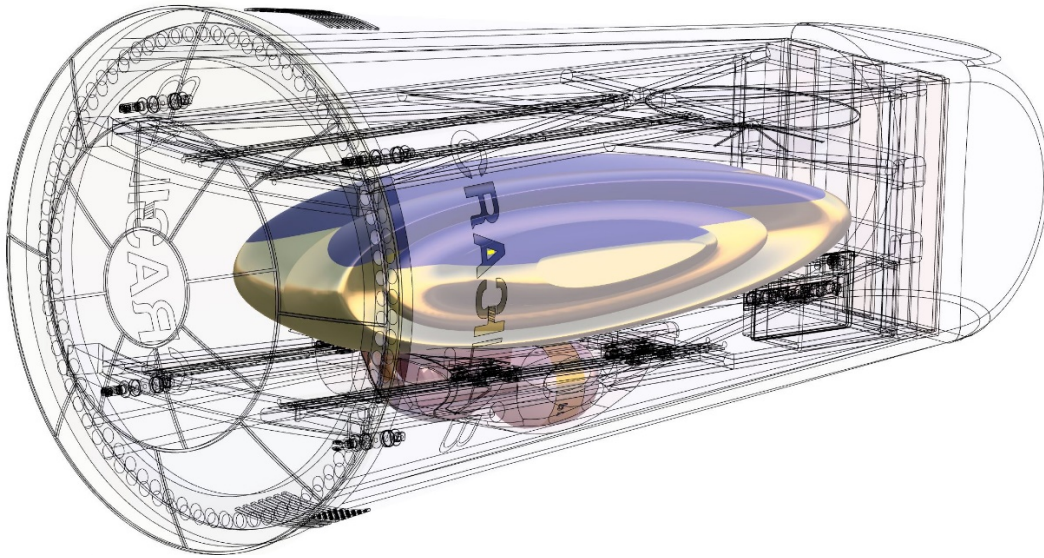


Figure 1: BREEZE packed in the entry vehicle

While BREEZE significantly expands on the capabilities of existing aerial vehicles designed to explore Venus, it is firmly built on technologies that are currently being implemented or under research by NASA. Altitude control for inflatable balloons has been well established and was implemented for Venus missions in 1985 [1]. However, bioinspired propulsion robots are a recent development, requiring significantly more complex mechanisms and control. Recent research, including the *CRASH* Team's own leading studies on cutting edge technology, has focused on addressing the complex controls, producing a number of prototypes for both in-air and in-water mobility [2-10]. In order to realize the BREEZE concept, a lightweight tension network must be developed to actuate the desired kinematics. The tension network illustrated in (Fig. 2b) would consist of cables running along the top and bottom of the wing, passing through the semi rigid wing ribs. This was inspired from the actual ray anatomy, illustrated in (Fig. 2c), which uses musculature to pull rigid cartilaginous links dispersed throughout their pectoral fins (wing-like lateral fins). Each top and bottom cable pair would be actuated independently to not only allow for a flapping motion but dynamic pitching. The tensioning actuators would be geared DC motors, whose power and efficiency scale well with mass [11], while they can also incorporate electroactive polymers, piezoelectric actuators, or supercoiled polymer actuators if those technologies become sufficiently developed. The use of many small actuators adds a level risk mitigation. If one of the actuators fails, the wing can still operate with a small power penalty. Furthermore, by placing all actuation components within the protective membrane of BREEZE, any possibility of exposure to the corrosive Venusian atmosphere would be eliminated. Tensioning cables could be run through sleeves attached to the inside of the membrane to remove any chances of cable tangling and snagging.

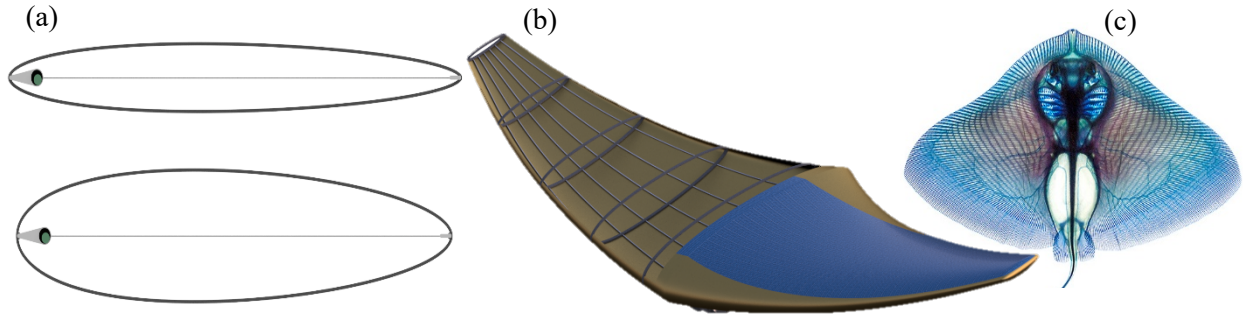


Figure 2: (a) Wing thickness expansion through the use of tensioning cable, (b) Cutaway of BREEZE skin showing tensioning cables used to pull on rib structures and, (c) Butterfly ray skeletal structure [12]

Volume reduction for buoyancy control can be achieved by pulling uniformly on top and bottom tensioning cables to shorten the span, while an alternate method would be to change the thickness of the vehicle (Fig. 2a). The latter method maintains the same wingspan allowing the solar panel area to remain constant, at the expense of added actuator mass. The required thickness change can then be achieved by using a tensioning wire to pull inward on the ends or top and bottom of the semi rigid ribs causing them to change area.

For charging, BREEZE will release its tension cables, allowing the vehicle to expand and rise to a higher altitude using buoyancy alone. When the vehicle is at a 50 km altitude, the clouds above block 50 to 80% of the incident solar radiation, as seen in (Fig. 3). However, as the vehicle rises to 60 km, it receives 70 to 80% of the maximum radiation. The flyer's top face will be equipped with soft solar panels. Although triple junction solar cell panels typically have higher efficiencies, NASA has made great progress with flexible solar panels. These flexible solar cells will better conform to the varying shape of the vehicle and reduce stress concentrations that could result from mounting the solar cells to the vehicle's outer membrane. Additionally, the use of flexible solar panels allows for the compact packaging of the vehicle for transit.

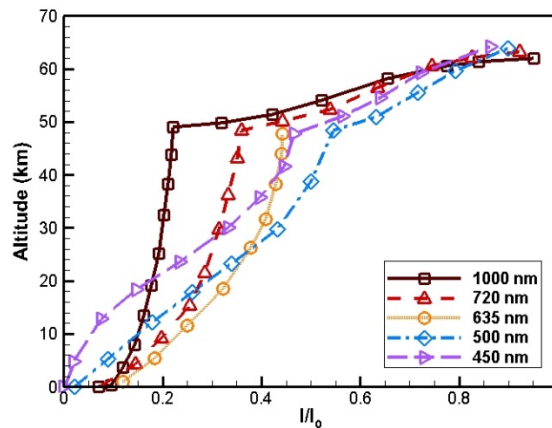


Figure 3: Solar radiation intensity of various wavelengths versus altitude [13]. Normalized intensity is relative to the max average solar flux of 2600 W/m^2

Recent advances in atmospheric balloon design has extended mission lifetimes by minimizing gas leakage. A recent study observed no measurable leakage after maintaining superpressure conditions for two weeks [14]. This long lifetime can be further extended by including extra tanks of lifting gas. Alternatively, it is also possible to harvest H₂O droplets which comprise 25% of the clouds in the target altitude [15] to perform electrolysis and produce hydrogen gas as suggested in a previous NIAC study [16]. A simpler alternative is to heat the in-situ atmosphere to replace the lost lifting gas. As the vehicle approaches the end of the mission, it will begin to sink into the warmer atmosphere. Before the mission is terminated, the vehicle can be plunged deep into the lower atmosphere to take high accuracy measurements of the lower atmosphere and terrain. Alternatively, the craft could be sent to the polar region on a mission to explore the polar vortices.

Once the technology has been developed for a single, large flyer, the concept could be scaled down to operate with many small-scale BREEZE family flyers. For the smaller vehicles, two or three flyers can be packaged together and deployed in a side-by-side formation to provide improved 3-D surface mapping via stereovision, as well as a larger field of view. Redundancy through the use of multiple flyers also lowers mission risk.

3. Mission overview

3.1. Earth to Venus Transfer and EDI

Based on analysis done using Systems Tool Kit (STK) a favorable launch date would be July 25th, 2034 at 09:54 UTC with a departure periapsis altitude of 185 km. The ΔV required would be 3.507 km/s for the transfer to Venus (Fig. 4). Transit time between Earth and Venus would take 146 days with a Venus arrival on December 18th, 2034 at 13:58 UTC.

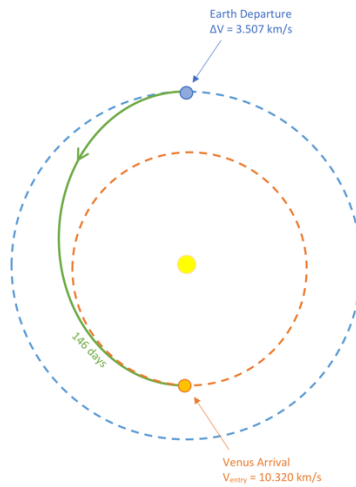


Figure 4: Earth to Venus transfer with a 146 day transit duration

The arrival periapsis altitude and velocity would be 500 km and 10.320 km/s, respectively. The entry, decent, and inflation (EDI) sequence would begin with the BREEZE vehicle stowed inside a 3.5 m diameter entry vehicle. The BREEZE entry vehicle will enter Venus' atmosphere on a ballistic trajectory at the equatorial plane (Fig. 5a). The entry system will utilize a Thermal Protection System (TPS) based on Heatshield for Extreme Entry Environment Technology (HEEET). Unlike HEEET, low to mid-density ablators such as PICA and AVCOAT would likely constrain the mission with steeper entry angles, higher peak dynamic pressures, and elevated heat fluxes. As the entry vehicle converges onto a subsonic velocity at (Fig. 5b), the rear aero cover will be released and 1 to 3 supersonic parachutes will be deployed for further deceleration (Fig. 5c). Once the entry vehicle has slowed sufficiently, the front heat shield will be dropped (Fig. 5d). BREEZE will then be released from the entry vehicle and start inflating (Fig. 5e). As BREEZE inflates its descent speed will be slowed further (Fig. 5f). Upon full inflation, the pressure canister used to fill the craft will be dropped (Fig. 5g) and BREEZE will rise.

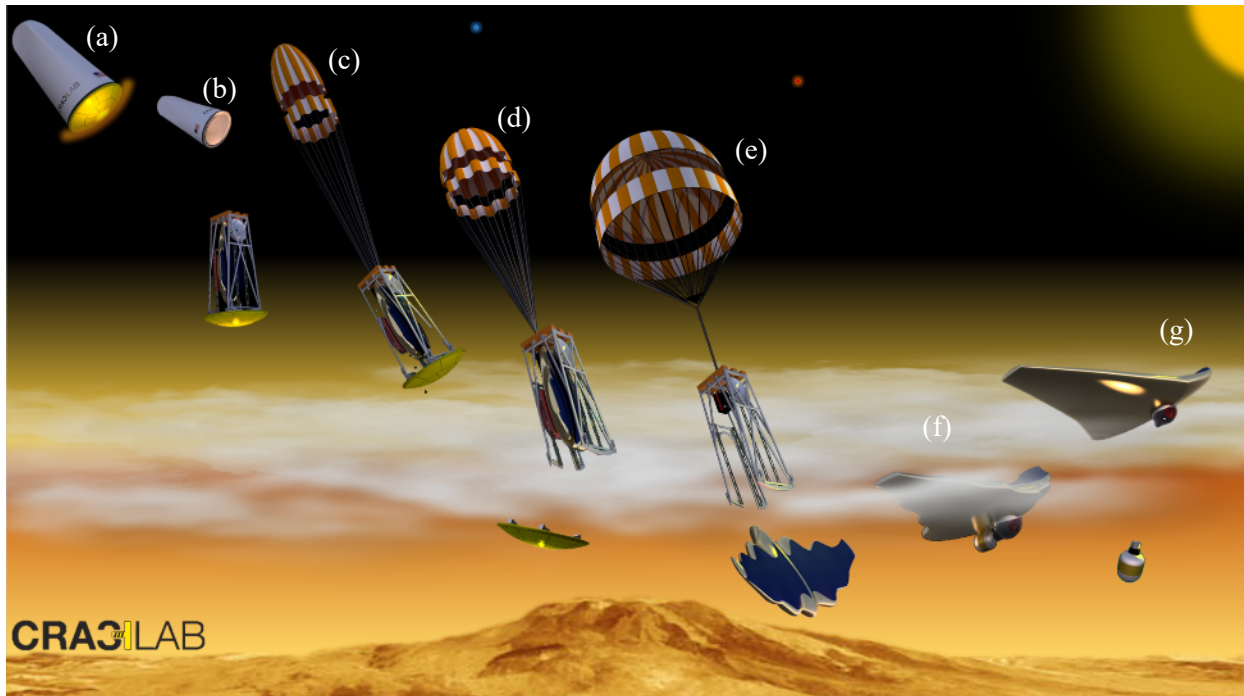


Figure 5: Entry, descent and inflation (EDI) sequence for BREEZE mission, (4a far left to 4g far right)

3.2. Operating Conditions and Flight Path

The BREEZE module will be designed to have a nominal altitude range from approximately 50 to 60 km. This specific range was selected because of the benign temperatures and pressures at these altitudes, but it can be extended for a limited time using the proposed bioinspired propulsion system. The nominal mission altitude straddles the thickest layer of the hazy atmosphere, allowing BREEZE to go to the low end

of the cloud layer to take measurements while still being able to reach the clearer section of the atmosphere for high-efficiency solar charging and propulsion.

For charging, the flyer will release its tension cables, enabling the vehicle to expand and rise to a higher altitude using buoyancy alone. When the vehicle is at its minimum operating altitude of 50 km, the clouds above block 50 to 80% of the incident solar radiation, but at 60 km, it receives 70 to 80% of the maximum radiation. The flyer's top face will be equipped with soft solar panels. Although triple junction solar cell panels typically have higher efficiencies, NASA has made great stride with flexible solar panels which would allow for increased wing range of motion and more compact packaging of the vehicle for interplanetary transit.

After EDI, the flyer will ride on the zonal winds. The wind speed at the target altitude is affected by the super-rotation of the atmosphere. Due to the extreme zonal wind speeds in the upper atmosphere of Venus as illustrated in (Fig. 6a), other lift based solar powered flyers are required to maintain speeds sometimes greater than 60 m/s to stay on the day side of the planet. If they traverse the night side of Venus, they risk an uncontrolled descent due to insufficient energy storage. However, because BREEZE is buoyant, it does not need to run its charge continuously to stay operational.

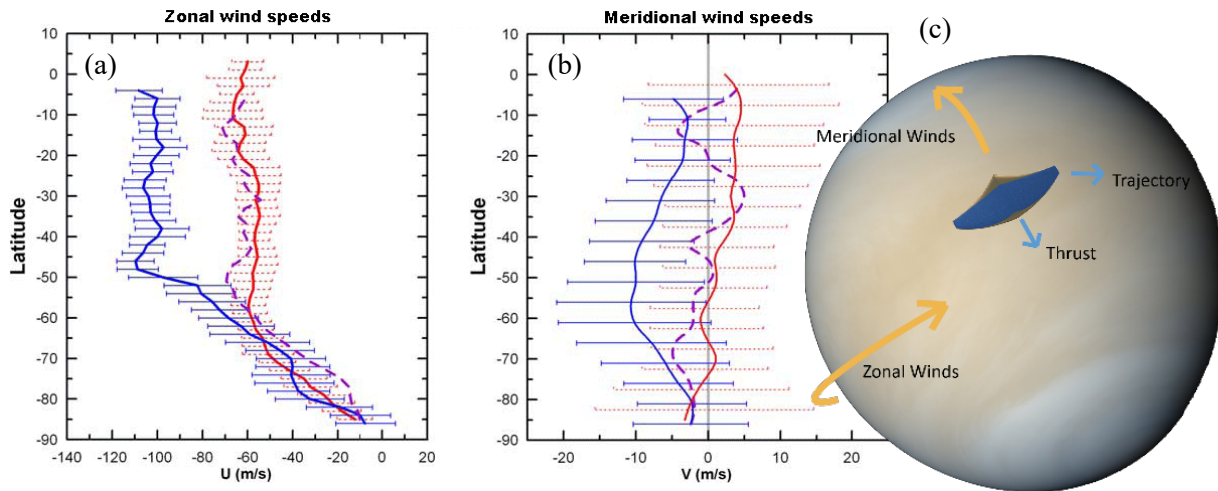


Figure 6: Zonal (a) and meridional (b) wind speed vs. latitude [17]. Both graphs show wind speed at three altitude ranges: 62-70 km (blue), 58-64 km (purple), and 44-48 km. (c) Trajectory of BREEZE as it circumnavigates the Venus via the assistance of the zonal winds

The super-rotation on Venus is dominated by the zonal winds, which can reach up to 80 m/s at an altitude of 60 km. The meridional winds are much more benign, peaking at approximately 5 m/s at the maximum target altitude (Fig. 6b). It is the meridional winds that blow atmospheric balloons toward the polar regions where they get trapped in polar vortices. BREEZE will be designed to propel itself and

counteract drift due to the meridional winds, while using the zonal winds to help it circumnavigate around the planet.

At BREEZE's operational altitudes, the zonal winds can circumnavigate the planet roughly every 4 to 6 Earth days. This provides 2 to 3 Earth days on the day side for charging. The flyer will be able to coast on the high winds as they carry it around the planet. This added efficiency enables BREEZE to charge during the day side and operate on the night side.

3.3. Instrumentation and Science Objectives

As BREEZE flies around the planet, it can use its scientific instruments to perform various atmospheric studies, while helping progressively improve the resolution of surface maps. Instrument selection of BREEZE is based on three references: The Venus decadal survey 2013-2022, Venus Exploration Analysis Group (VEXAG) research, and the BREEZE Team's science mission studies. The highest priority instruments are: a mass spectrometer, Radar, a solid-state magnetometer, and Thermal Emission Imaging System (THEMIS).

On-board instruments have different purposes and collect data at different times as BREEZE flies around Venus. The flyer will dip into the atmosphere where a mass spectrometer will take samples of the Venusian atmosphere in order to measure mass to charge ratios of molecules, and to determine their molecular mass. Data collected from the mass spectrometer will also show isotopes present in the atmosphere. This information will help study the history of climate evolution on the planet. A mass spectrometer meets a high total of seven of the decadal survey goals and objectives, making it the highest priority instrument. On BREEZE, Radar will obtain high-resolution imaging during flyover in order to study weather, potential volcanic activity, and tectonic faulting.

Unlike Earth, Venus does not have an intrinsic magnetic field, it has what is referred to as an "induced magnetosphere", caused by ionization between Venus' upper atmosphere reacting with solar wind. BREEZE will contain a solid-state magnetometer which will take constant readings of magnetic field. The last primary instrument BREEZE will carry is a THEMIS for surface imaging. The THEMIS captures both visible and infrared reflections from the surface enabling mapping of different mineral concentrations. During mission end of life, BREEZE will slowly leak helium and descend to the surface allowing for even higher resolution imaging.

Instruments of secondary priority are a gamma ray spectrometer, an ultraviolet spectrometer, a nephelometer, and an x-ray diffractometer. When BREEZE dips to its lowest altitude, a gamma ray spectrometer (GRS) will take readings to determine abundance of elements on the surface. The GRS will turn on and off as the vehicle rises and falls. During both rise and fall, an ultraviolet spectrometer (UVS)

will determine the distribution of atoms and ions that are present with changes in altitude. During the time when GRS is taking readings, UVS will begin to determine ultraviolet scattering properties of the lower planetary atmosphere. Both the nephelometer and x-ray diffractometer, similar to the UVS, will measure the concentration and size of particles in the lower atmosphere, through using the light they emit. Having been equipped with these different types of instruments will offer BREEZE a means of comparison to help obtain the highest quality of data.

BREEZE will further have the potential to discover extraterrestrial life on Venus. Climate simulations conducted by NASA's Goddard Institute for Space Studies show Venus could have supported a shallow liquid-water ocean and habitable surface temperatures for up to two billion years of the planet's early history. Although life is unlikely to exist at the surface today, it is possible microbial life exists in Venus' atmosphere. The lower cloud layer (47.5-50.5 km), which is partially within BREEZE's operational altitude, hosts comparable temperatures and pressures to those found on Earth, as well as abundant sulfuric acid aerosols [18]. Certain sulfur allotropes, particularly octasulfur, could be used by microbes as a UV sunscreen, an energy converting pigment, to convert UV radiation to lower frequencies for photosynthesis [19]. Additionally, the transmission spectra for the Iro protein, involved in iron respiration in the acidophilic and sulfur-metabolizing bacterium *Acidithiobacillus ferrooxidans*, has compelling overlap with Venus' albedo [18]. *Acidithiobacillus ferrooxidans* is an extremophile naturally found in iron sulfide deposits, thriving in 60 °C and 1-2 pH environments where it oxidizes iron and sulfur for energy. Recent observations suggest Venus is volcanically active, possibly seeding the atmosphere with the nutrients necessary for a mega colony of iron and sulfur metabolizing micro-organisms.

Evidence for biological activity can be best found by in situ observations of bio-signatures. Several instruments have demonstrated bio-signature detection capabilities, including the acousto-optic tunable filter (AOTF) IR reflectance spectrometer, laser desorption/ionization time of flight mass spectrometer (LD-TOF-MS), laser-induced breakdown spectrometer (LIBS), and scanning electron microscope. These instruments could be included as an alternate payload for BREEZE.

4. Bioinspired Propulsion Analysis

The aerodynamic analysis of the system was conducted using a computational fluid dynamics (CFD) approach. The CFD analysis provided quantitative and qualitative evidence of BREEZE's thrust generation mechanism. BREEZE performs twisting and flapping across its span in order to propel itself in the forward direction. Inviscid and laminar fluid flow modeling was used to carry out the analysis. The numerical method, kinematics of BREEZE's flapping motion, and results of different parametric studies are discussed in this section.

4.1. Numerical Methods

The unsteady Navier-Stokes equations were employed to resolve the flow around BREEZE. Assuming incompressible laminar flows, the continuity equation is:

$$\nabla \cdot \vec{v} = 0 \quad (1)$$

Where, \vec{v} is the velocity vector and ρ is the fluid density. Neglecting gravitational effects, the momentum equation is:

$$\rho \left[\frac{\partial(\vec{v})}{\partial t} + \vec{v} \nabla \cdot \vec{v} \right] = -\nabla p + \nabla \cdot \vec{\tau} \quad (2)$$

For the 3-D simulations, a fully coupled, pressure-based approach [20] was used to solve the momentum equations. The simulations used a coupled approach to solve for pressure-velocity coupling, least square based approach to solve for gradients, and second-order scheme to solve for pressure and momentum. The time marching in simulations was done using the first-order scheme. The convergence criteria for the all variables were set to 1e-6 to ensure accuracy.

An efficient meshing strategy was required to allow for proper mesh resolution due to the large displacement associated with the flapping motion of BREEZE in three dimensions. Overset meshing was chosen in order to retain mesh resolution and to create separate meshes associated with geometric variations. The overset meshing approach used overlaying mesh regions for the background and components (component is in this case is the BREEZE module). Component meshes for BREEZE could overlap one another arbitrarily, with multiple meshes combined to form the full module as long as the physical boundaries did not intersect. The BREEZE component mesh with an enclosure is shown in (Fig. 7). The BREEZE motion includes flap and twist across its wing span. Hence, the overset mesh avoids re-meshing flaws and setup issues related to a large displacement of mesh. The mesh used in the simulation is several times finer than what is shown in (Fig. 7a). The component mesh includes the inflation layers near the surface. The inflation layers allow for the capture of boundary layer effects. The overset mesh developed overlaps the background mesh, consisting of hexahedral cells. The component domain on the other hand consists of tetrahedral cells, representing a typical BREEZE module simulation with around 3 million cells.

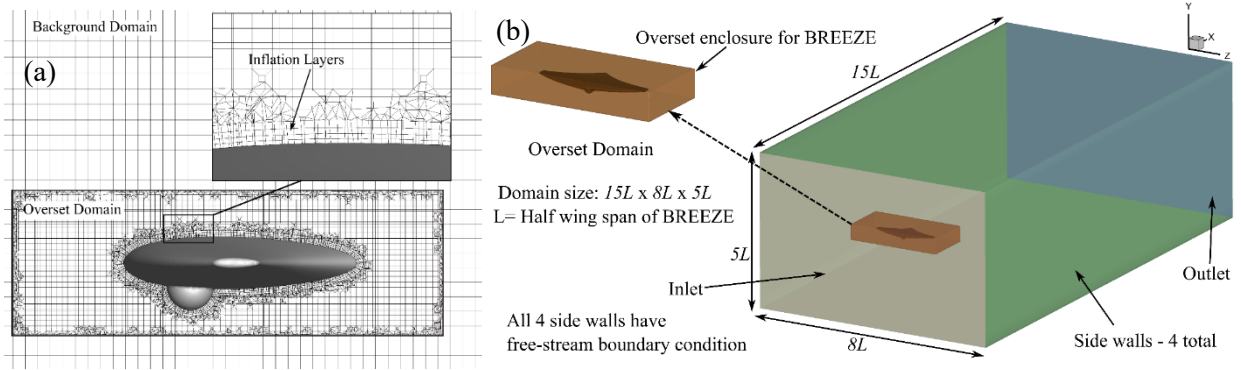


Figure 7: (a) Overset domain of background and component with inflation layer on BREEZE surface.
 (b) Computational domain used in the simulations along with the selected boundary conditions

The domain used for computational framework is shown in (Fig. 7b). The domain size is given with reference to the BREEZE’s half span length ($L=5$ m). The domain size is therefore $15L \times 8L \times 5L$. BREEZE is located at $2L$ distance from the inlet. All four side walls have free-stream boundary condition. The domain size is chosen to be large enough to remove any wall effects. The fluid density was taken as the density of carbon dioxide.

4.2. Kinematic Parameters

BREEZE mimics the behavior of stingray for thrust generation [21], performing twisting and flapping. The flap and twist motions occur simultaneously as shown in (Fig. 8a). The twist motion is carried out about the Z-axis i.e., spanwise direction, where the flapping occurs in YZ plane i.e., about the X-axis. The flap and twist at every location are governed by Eqs. (3) and (4). They are both a function of the ratio of span location and half span (Z_{\max} or L). The distribution of flap and twist varies with a power of 1.5. The flap amplitude (A_y) depends on Strouhal number (St). The twist amplitude (A_θ) depends on relative angle of attack (AOA) [22]. Eqs. (3) and (4) dictate that BREEZE has the highest twist and flap amplitude near the tip and zero amplitude towards its root.

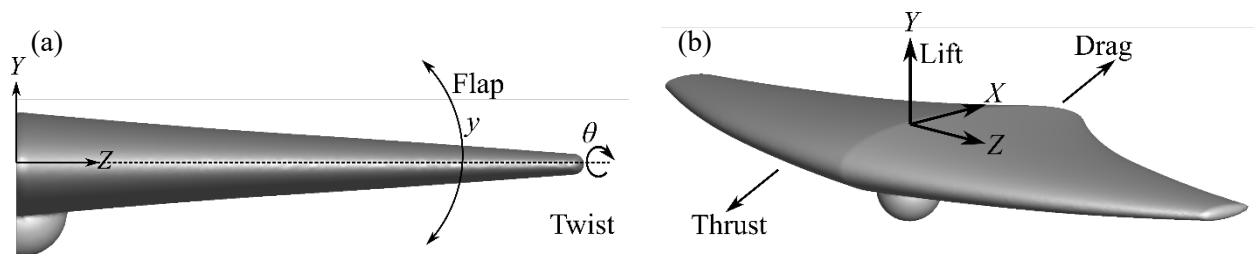


Figure 8: (a) Flap amplitude and twist angle direction in BREEZE kinematics, (b) direction of forces and 3-D axis orientation in simulations

$$y(z, t) = \left[\frac{z}{Z_{max}} \right]^{1.5} A_y \sin(2\pi ft) \quad (3)$$

$$\theta(z, t) = \left[\frac{z}{Z_{max}} \right]^{1.5} A_\theta \sin(2\pi ft) \quad (4)$$

The time history of flap and twist amplitudes based on Eqs. (3) and (4) at the different span locations are shown in (Fig. 9a) and (Fig. 9b). It is evident that the wing tip experiences maximum twist and flap, similar to that of the stingrays. The twist and flap amplitudes decrease from tip to root.

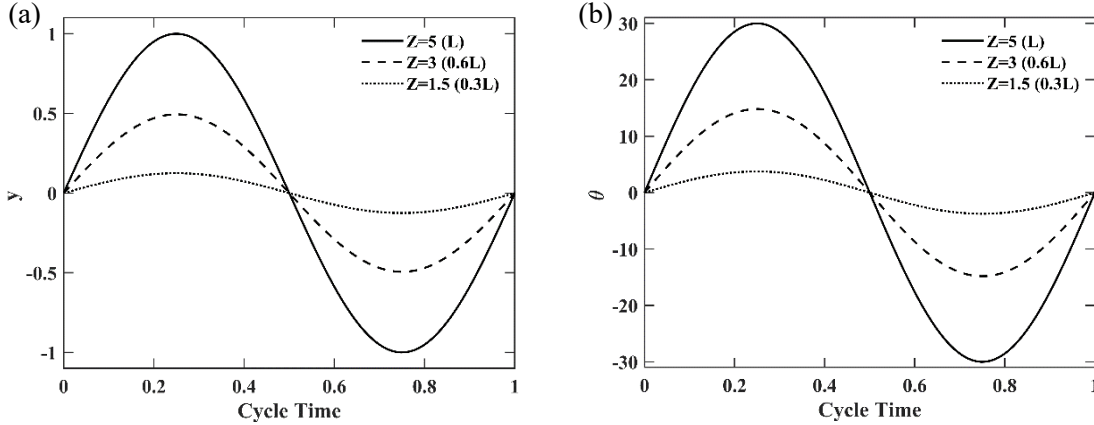


Figure 9: (a) Flap amplitude of 100% (tip), 60% and 30% span location in a cycle. $(A_y)_{max} = 2$ m at tip, (b) twist amplitude of 100% (tip), 60% and 30% span location in a cycle. $(A_\theta)_{max} = 30^\circ$ at tip

The Strouhal number is a dimensionless parameter that can be used to describe unsteady aerodynamics of a flapping flight. The Strouhal number governs the characteristics of propulsive nature and vortex shedding behind the body in most natural flyers. The Strouhal number is defined as the ratio of oscillating speed (fA) to forward speed (U) i.e., $St = fA/U$ where f is flapping frequency and A is flap amplitude. Flyers and swimmers in nature tend to have Strouhal number between 0.2 and 0.4 [23]. The propulsive efficiency is also high in this range. Hence, in order to get the most thrust and highest efficiency from BREEZE, it will need to operate within this range. The Strouhal number is also important in the calculation of the relative AOA. Wing twisting motion is a particular feature of BREEZE's flapping as indicated earlier. The twisting motion is thought to have a significant impact on thrust. To determine the influence of twisting, the relative AOA is calculated for each span location (Fig. 10). The flap velocity associated with each span location is different based on flap amplitude calculated from Eq. (3). Further, the twist at every span location is different based on twist amplitude calculated from Eq. (4). Therefore, the relative AOA (α) defining twist at each section can be calculated using Eq. (5):

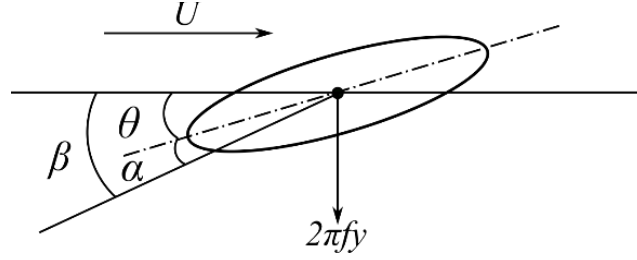


Figure 10: Relative angle of attack (AOA) at any span location.

$$AOA = \tan^{-1}\left(\frac{2\pi fy}{U}\right) - \theta, \text{ where } \beta = \tan^{-1}\left(\frac{2\pi fy}{U}\right) \quad (5)$$

Table 1: Kinematic parameters of the flapping flight associated with BREEZE

f (Hz)	A (m)	U (m/s)	St	T (Cycle time)	θ (°)	α (°)
0.5	2	5	0.2	2	12.1	20
0.75	2	5	0.3	1.333333	23.3	20
1	2	5	0.4	1	31	20

The amount of thrust produced by BREEZE increases with higher AOA. However, high AOA may cause stall and give rise to drag. Hence, it is essential to calculate the relative AOA for every Strouhal number. The Table 1 shows the governing parameters associated with different Strouhal number for an amplitude of 2 m for tip location ($L=5$) of BREEZE. The parameters given are for a fixed relative AOA of 20°. It is also evident that the twist angle increases with rising Strouhal number. Hence, for the same relative AOA, higher twist is required. It is important to note that relative AOA and twist both decrease from tip to root.

Using the BREEZE analysis, the coefficients of forces can be determined. The lift and drag forces are normalized by multiplying them by $\frac{2}{\rho U^2 A}$, where $U=5$ m/s (incoming free stream velocity) and A is the surface area of BREEZE. It is important to note that negative drag is equivalent to thrust as shown in (Fig. 8b).

4.3. CFD Results and Discussion

The flapping cycle starts from the top of the downstroke (uppermost location of the wingtip), as shown in (Fig. 11a). The wing undergoes a downstroke (moving from maximum amplitude to minimum amplitude) between non-dimensional cycle time $T=0$ to 0.5 and upstroke between $T=0.5$ to 1.

The bioinspired mechanism of stingray was implemented as shown in Fig. 11. The amplitude of oscillation was kept 2 to 2.5 m for realistic deformation of wing. Based on the pressure contours shown in Fig. 11, it is evident that the high pressure region is mainly confined to the leading edge of BREEZE. During the point of maximum thrust production of downstroke (Fig. 11c), the high pressure region is located on the bottom of BREEZE's surface due to the downward motion of the wing, where flow pushes the wing toward the forward direction. Whereas for the upstroke (i.e Fig. 11g) the higher pressure region moves towards the top surface, where flow now propels the wing again in the forward direction due to upward motion and vortex structures formation near the leading edge. The solid physics and versatility of BREEZE are clearly visible and intriguing based on the preliminary results shown.

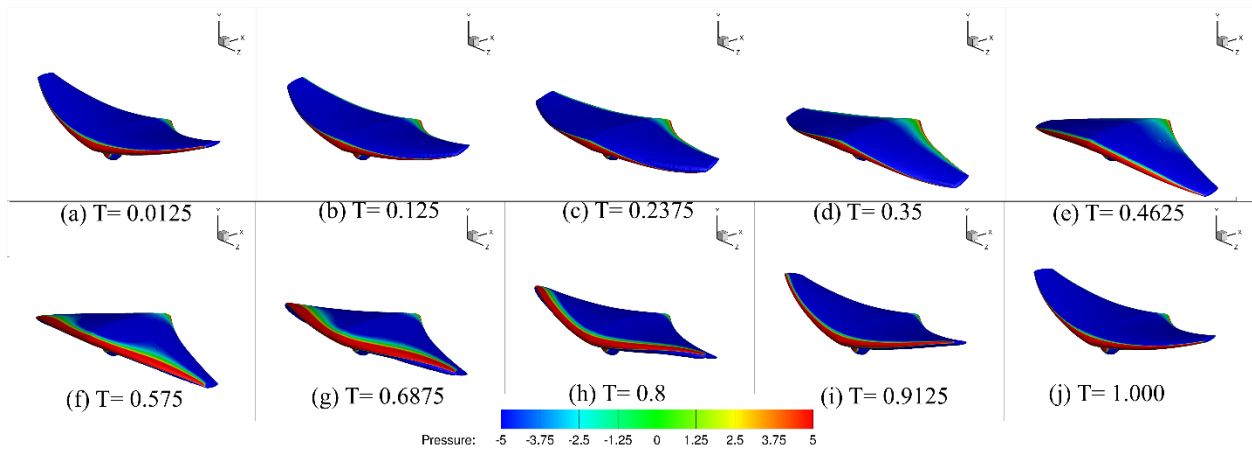


Figure 11: Pressure (Pa) contours on BREEZE surface during one cycle from (a) $T=0.0125$ to (j) $T=-1.00$ for $St=0.3$ and relative angle of attack of 20°

The aerodynamic analysis of BREEZE consists of four different parametric studies. In the first study, inviscid modeling was compared against the laminar modeling. In the second study, the effect of different relative AOA was examined. In the third study, the impact of flap amplitude on thrust production was considered. Finally, the last study focused on how Strouhal number affects aerodynamic forces.

Since the whole propulsion study presented in this report is focused on the basic fluid modeling around BREEZE when it operates in Venus' upper atmosphere, it is essential to compare the inviscid and laminar flow models. It is known that inviscid modeling reduces the computational cost associated with simulations. If inviscid modeling provides a good approximation of aerodynamic parameters compared to laminar study, then it can be used effectively to conduct a more in-depth and wide parametric study on BREEZE.

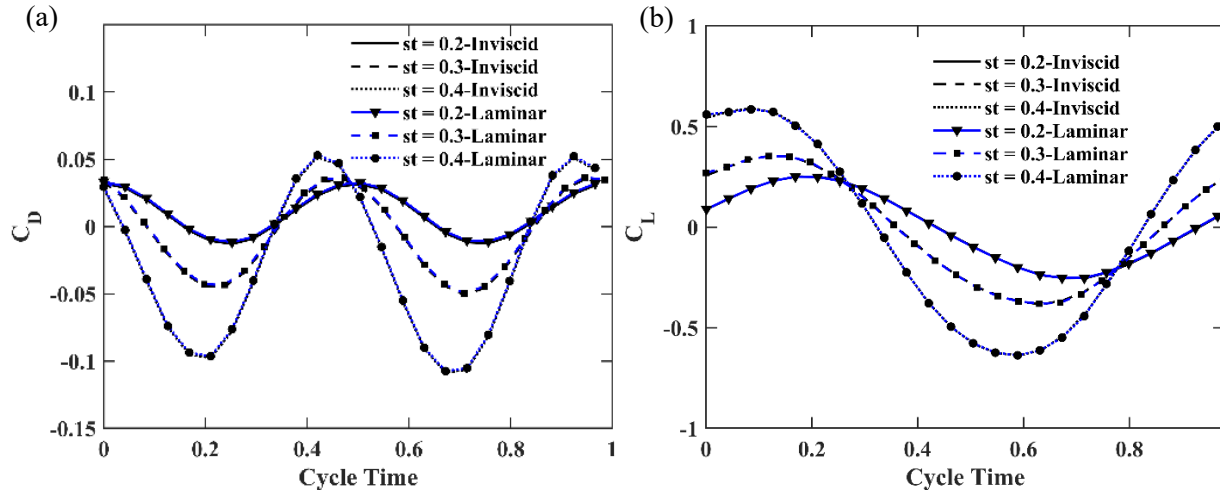


Figure 12: (a) Coefficient of drag for $St=0.2, 0.3$ and 0.4 for inviscid and laminar flow modeling, (b) coefficient of lift for $St=0.2, 0.3$ and 0.4 for inviscid and laminar flow modeling

The coefficient of lift and drag are shown in Fig. 12. The force-time history is determined for three Strouhal numbers of 0.2, 0.3 and 0.4. The amplitude for all Strouhal numbers was fixed at 2 m and the relative angle of attack was fixed at 20° for all Strouhal numbers. The same flap and AOA present a great comparison for the laminar and inviscid modeling. The cyclic average values represent the average of forces throughout the periodic motion of BREEZE’s flapping, i.e. when the wings come back to the same position after a flap. The difference in cyclic average values are presented in Table 2. The cyclic average values give insight into the difference of total lift and thrust production in a cycle.

Table 2: Difference in cyclic average lift and drag values for Strouhal number 0.2, 0.3 and 0.4

St	$\Delta \overline{C_D}$	$\Delta \overline{C_L}$
0.2	0.001255	8.59935E-05
0.3	0.001241	0.00033851
0.4	0.001301	0.00027376

The cyclic average values show that at $St=0.2$ the lift is near zero for both inviscid and laminar models. The drag for $St=0.2$ in laminar and inviscid is quite similar. The lift at all Strouhal number is identical in both inviscid and laminar modeling. The overall force-time trend shown in Figs. 12a and 12b provides visual evidence of similar forces from both methods of modeling. Specifically, at $St=0.4$, the lift and thrust are quite identical. This behavior states that inviscid modeling provides accurate results and can be used for

computational modeling. This allows for more cases to be run when computational resources are limited as is often the case.

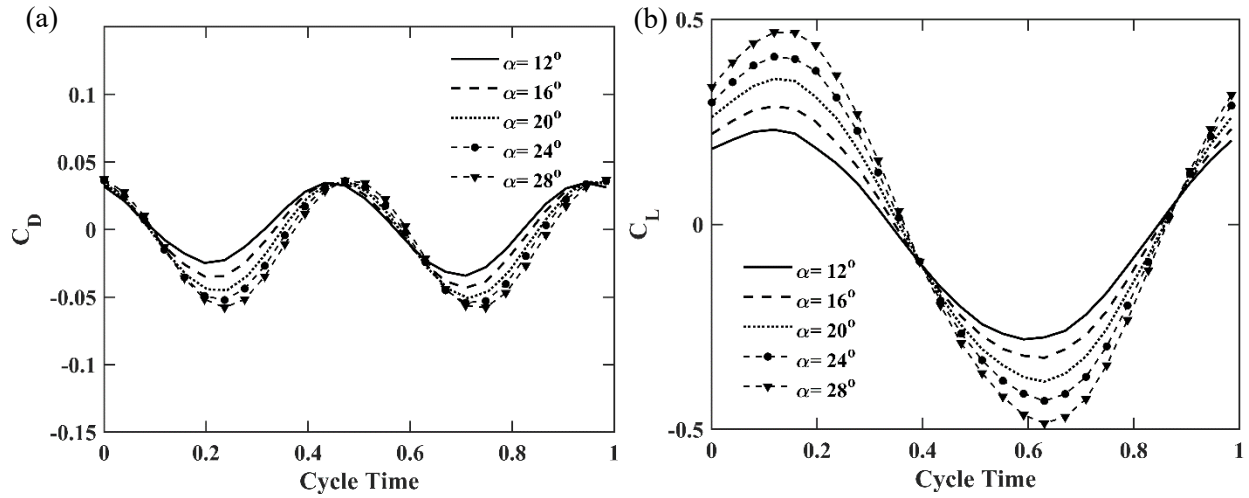


Figure 13: (a) Coefficient of drag for different relative AOA for Strouhal number 0.3 and $A=2m$, (b) coefficient of lift for different relative AOA for Strouhal number 0.3 and $A=2m$

The second parametric study was carried out on the effect of the relative angle of attack at a particular Strouhal number of 0.3. The flap amplitude was kept constant at 2 m. The relative AOA values presented in Figs. 13a and 13b are maximum relative AOA at the tip. The maximum twist angle applied at the tip is shown in Table 3 along with AOA and cyclic average lift and thrust values. It is evident that except for the case of 12° AOA, every AOA generates thrust. The thrust increases with the relative AOA. The drastic increase in thrust is between 16° and 20° , where the thrust increase from 0.00133 to 0.00511. The thrust increases steadily between 20° to 28° from 0.00511 to 0.00943. In all cases, there is a slight negative lift, i.e. downward force to decrease altitude of BREEZE. The negative lift is likely due to the flow accelerating around the payload module. The negative lift is not a concern as buoyancy force will compensate for any slight negative lift produced.

Table 3: Cyclic average lift and drag values at various relative angles of attack

$\alpha_{max}(\text{°})$	$\theta_{max}(\text{°})$	$\overline{C_D}$	$\overline{C_L}$
12	31.3	0.002924	-0.01508
16	27.3	-0.00133	-0.01144
20	23.3	-0.00511	-0.00792
24	19.3	-0.00753	-0.00401
28	15.3	-0.00943	-0.0012

Figure 14a shows the comparison of pressure distribution on the bottom BREEZE surface for the lowest AOA of 12 and the highest AOA of 28. The high pressure region at mid downstroke ($T=0.25$) is larger for the AOA 28 case and explains the higher thrust and lift. Similar to manta rays, BREEZE generates the majority of thrust from tip pressure distribution. Figure 14b shows the Z-vorticity at 80% location on the BREEZE wingspan. The red (positive) and blue (negative) vorticities represent the clockwise and counter-clockwise vortex structures, respectively. The larger vortex structures in AOA 28 gives visual evidence of higher force production in high AOA cases.

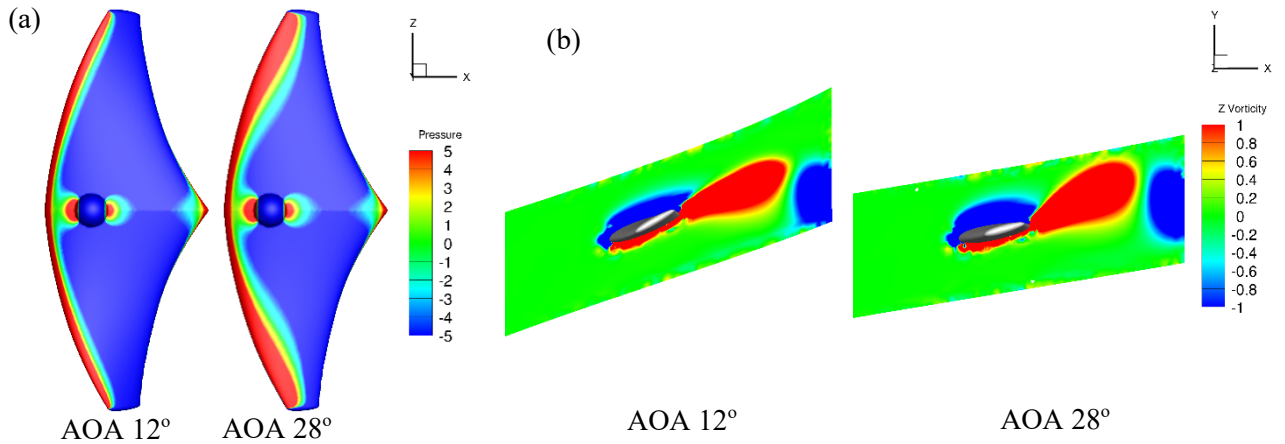


Figure 14: (a) Pressure contours on bottom of BREEZE surface at time $T=0.25$ and $St=0.3$, (b) Z-vorticity (spanwise vorticity) at span location of 80% ($0.8L$) at $T=0.25$ and $St=0.3$

The third parametric study conducted was the effect of flap amplitude on drag and lift. Strouhal number ($St = fA/U$), as well as the freestream velocity, were kept constant. In order to keep Strouhal number constant, the frequency had to be varied inversely to amplitude. The cyclic thrust and lift for different amplitudes at a constant Strouhal number are shown in Fig. 15.

Table 4: Cyclic average lift and drag values at various amplitudes and $St=0.3$ and relative AOA of 20°

A (m)	$\overline{C_D}$	$\overline{C_L}$
1	0.007007	-0.0073
1.5	-0.00011	-0.01045
2	-0.00511	-0.00792
2.5	-0.00753	0.001569

The mean coefficient of thrust values for 1.5, 2 and 2.5 m were calculated as 0.00011, 0.00511 and 0.0075 (~ 4.4 N) as shown in Table 4. The amplitude of 1 m yields net drag production with a coefficient of drag of 0.007. It is also evident that with increasing amplitude, the variance of lift decreases. These results are promising and show that a higher amplitude and lower frequency can lead to a stable and energy-efficient system.

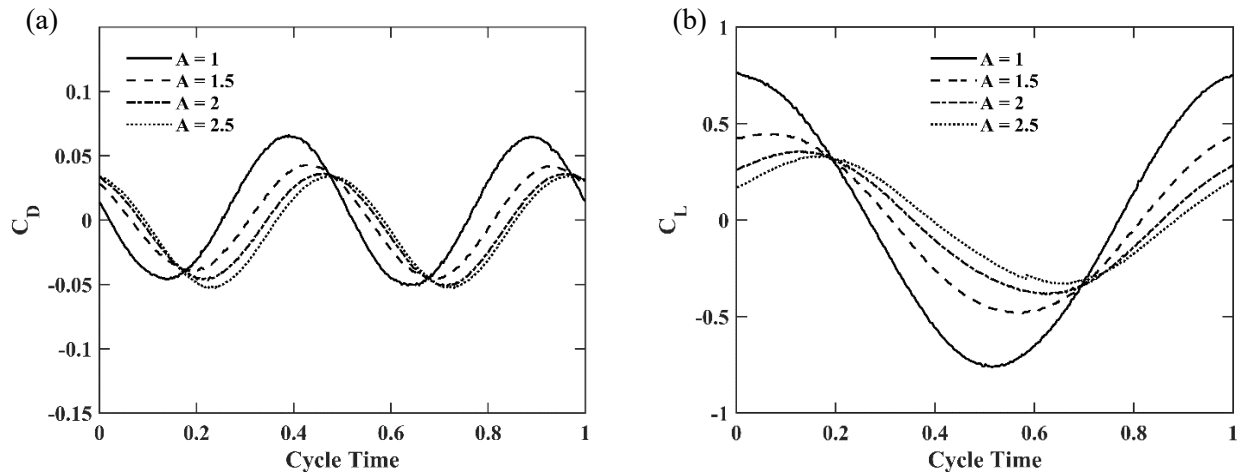


Figure 15: (a) Force-time history of thrust during one flapping cycle of BREEZE for different oscillation amplitude at $St=0.3$, (b) force-time history of lift during one flapping cycle of BREEZE for different oscillation amplitude at $St=0.3$

The last parametric study conducted was the effect of Strouhal number on the aerodynamics of BREEZE. To vary the Strouhal number, the frequency was varied while flap amplitude and freestream velocity were kept constant. The time history of the coefficient of drag and coefficient of lift for three Strouhal number of 0.2, 0.3 and 0.4 are shown in Fig. 16.

Table 5: Cyclic average lift and drag values at various Strouhal number, $A=2$ m and relative AOA of 20°

St	$\overline{C_D}$	$\overline{C_L}$
0.2	0.009767	0.000137
0.3	-0.00511	-0.00792
0.4	-0.02639	-0.01436

It is evident that for Strouhal numbers of 0.3 and 0.4, there is net thrust production in a cycle. However, at a Strouhal number of 0.2, there is no thrust production (coefficient of drag ~ 0.009). The mean values of the coefficient of thrust in a cycle were calculated as 0.0051 and 0.02639 for the Strouhal number of 0.3 and 0.4 as shown in Table 5.

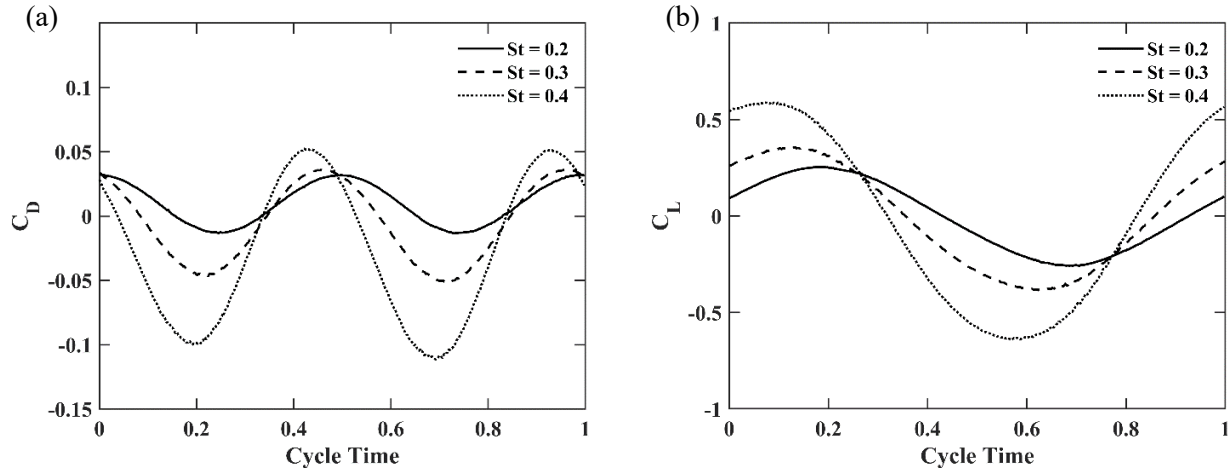


Figure 16: (a) Force-time history of thrust during one flapping cycle of BREEZE at different Strouhal number, (b) force-time history of thrust during one flapping cycle of BREEZE at different Strouhal number

Figure 17a shows the comparison of pressure distribution on the bottom BREEZE surface for a Strouhal number of 0.2 and a Strouhal number of 0.4. It is clear that at a Strouhal number of 0.4 the high pressure region is larger near wingtip and extends further towards the trailing edge. However, the Strouhal number of 0.2 shows very uniform pressure gradients in the spanwise and chordwise direction. Figure 17b shows the Z-vorticity at 80% span location of the BREEZE wing. The vortex structures are more frequently shedding when Strouhal number is 0.4 then when Strouhal number is 0.4. The clockwise vortex is more stretched in a Strouhal number of 0.2 and the counter-clockwise vortex is smaller compared to a Strouhal number of 0.4. The vortex structures at a Strouhal number of 0.4 are larger compared to a Strouhal number of 0.4. Hence, larger and frequent vortex shedding gives rise to higher thrust in at a Strouhal number of 0.4.

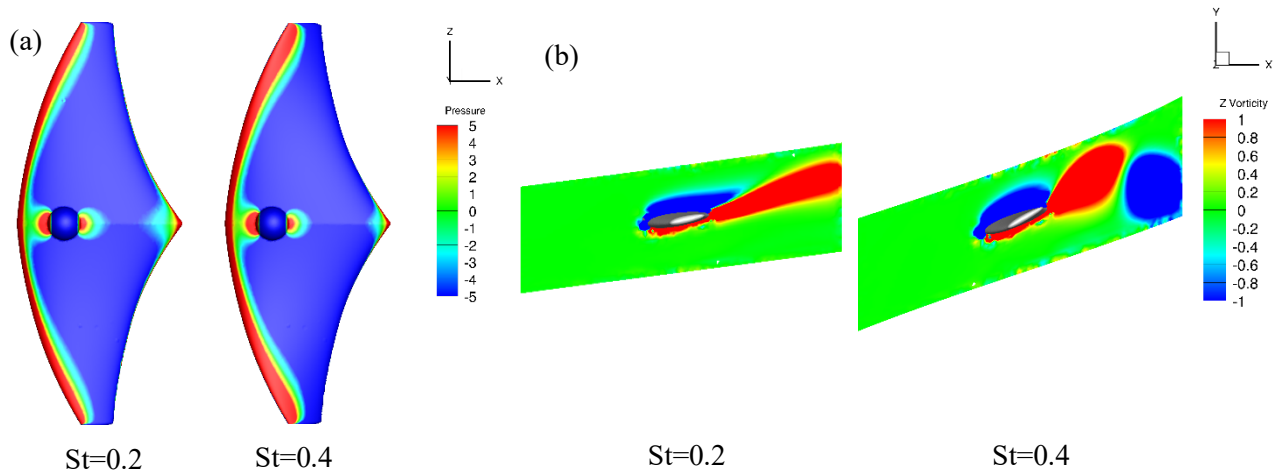


Figure 17: (a) Pressure contours on bottom of BREEZE surface at time $T=0.25$ and $A=2$ m, (b) Z-vorticity (spanwise vorticity) at span location of 80% ($0.8L$) at $T=0.25$ and $A=2$ m

The iso-surfaces of the Q-criterion at level 1 for a Strouhal number of 0.2 and 0.4 are shown in Fig. 18. Iso-surfaces of the Q-criterion illustrate vortex behavior in 3-D. The Strouhal number of 0.2 shows stretched vortices in the wake, while the Strouhal number of 0.4 leads to denser and larger vortex structures forming within the wake.

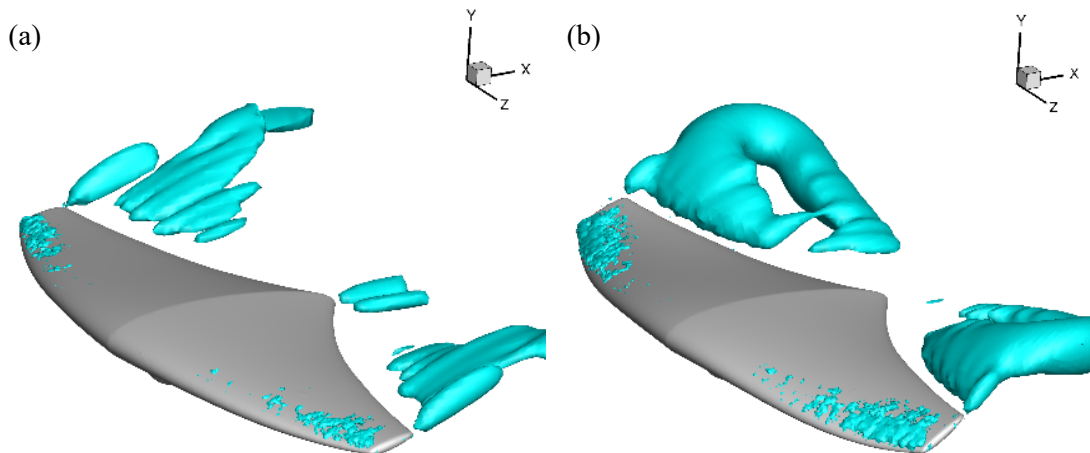


Figure 18: Iso-surfaces of Q-criterion at level 1 for $St=0.2$ (a) and $St=0.4$ (b)

In brief, the parametric studies of AOA, flap amplitude, and Strouhal number show that BREEZE's bioinspired propulsion can generate net thrust at speeds of 5 m/s allowing it to make headway against Venus' meridional winds. BREEZE sheds tip vortices with higher frequency to maintain necessary net thrust. Increasing the size of the high pressure region at BREEZE's wingtip can be done by increasing flap amplitude, AOA, and Strouhal number. A large high pressure region at the wingtip will result in stronger thrust production and vortex shedding.

5. Flight Dynamics and Stability

5.1. Modeling Methods

A MATLAB environment was created to study BREEZE’s flight dynamics and flight stability. The program can calculate BREEZE’s trajectory and longitudinal stability during flight (Fig. 19), but also identify BREEZE’s lift, thrust, and plot flight trajectory based on BREEZE’s self-propulsion.

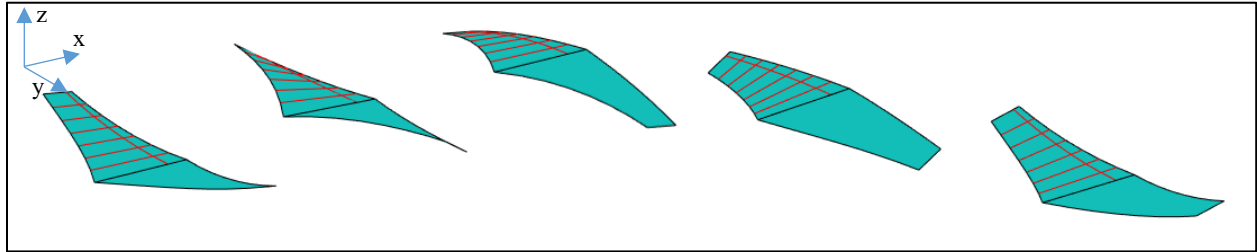


Figure 19: BREEZE flight trajectory time-lapse computed in Matlab environment (not to scale for visual clarity)

MST (Modified Strip Theory, an empirical aerodynamic model) was used to calculate aerodynamic forces, while basic kinematic equations govern BREEZE’s movement. The Matlab program architecture is represented by the flow chart in shown in Fig. 20. Due to the computationally inexpensive nature of this environment, it can be used to conduct a parametric study on a number of BREEZE’s parameters, including planform geometry, wing kinematics, and mass and lifting gas distribution. In future work, a trade space could be created to determine the best BREEZE dependent on decisions on power requirements, mass requirements, and/or shape constraints.

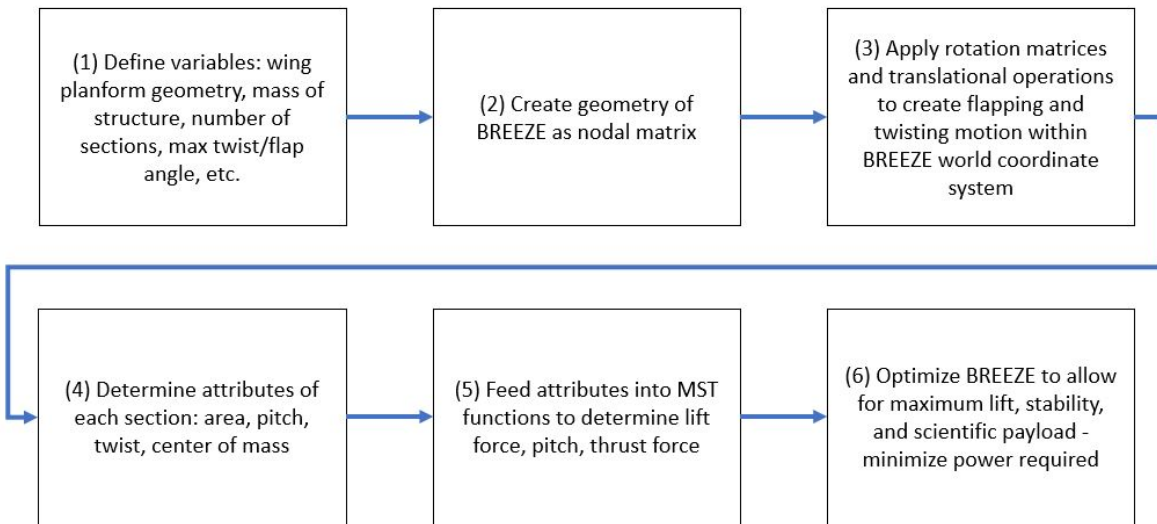


Figure 20: Matlab Flight Dynamics and Stability Program Architecture

The program was created using a strip by strip approach for both geometric modeling of BREEZE within the simulation and application of aerodynamic forces on the flyer. The assumption being made is that when examining forces on enough discretized small strips of the wings (Fig. 21b), the results are close to what the actual nature would be [24].

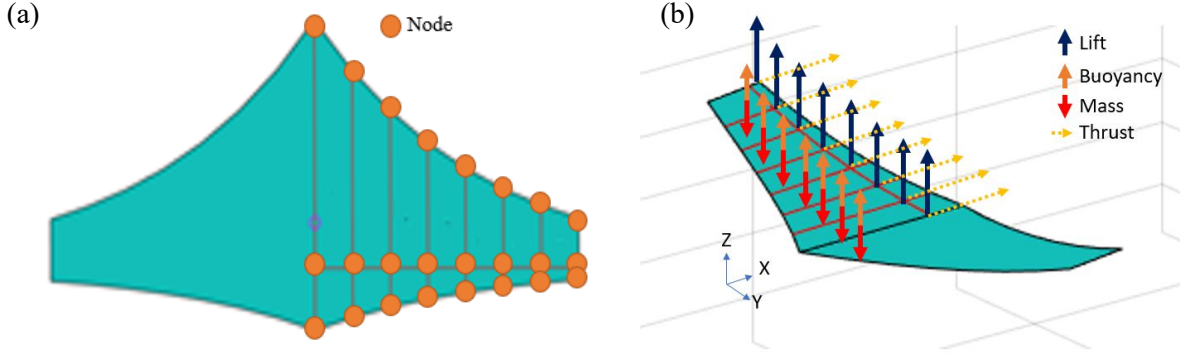


Figure 21: (a) Planform geometry and nodal locations, (b) simplified forces acting on BREEZE

To break the wing into strips, BREEZE is modeled in Matlab as a nodal matrix (Fig. 21a) with offset sinusoidal functions to govern the flapping and twisting of the wings (max twist at zero flap angle and vice versa); matrix rotations and translations allow for BREEZE to illustrate its flight and create nodal data required for calculating aerodynamic forces.

Seen in Fig. 21a is BREEZE from the top-down cross section (planform view). Each of sections can be seen separated by red lines. Based on the flapping motion observed within the global coordinate system in the simulation, data is fed into a group of functions that are then able to produce lift and thrust estimates for each section. These forces are found on a strip-by-strip basis and are then applied to the center of the section if it is a lift or buoyancy force and to the quarter-chord of the section if it is a lift or drag force [24]. Equations (6) and (7) give sectional lift and thrust forces, while Eqs.(8) and (9) give total lift and thrust force acting on BREEZE:

$$dL = (F_n + F_a) \cos(\theta_s) + (F_s + F_c + F_f) \sin(\theta_s) \quad (6)$$

$$dT = (F_s + F_c + F_f) \cos(\theta_s) - (F_n + F_a) \sin(\theta_s) \quad (7)$$

$$Lift = 2 \int_0^S \sin(\gamma) dL \quad (8)$$

$$Thrust = 2 \int_0^S dT \quad (9)$$

Where dL is total sectional lift, dT is total sectional thrust, θ_s is the sectional pitch angle (the summation of body pitch and wing twist), F_n is the sectional force perpendicular to chord due to fluid circulation, F_a is sectional force perpendicular to chord due to apparent mass effect, F_s is sectional force parallel to chord

from leading edge suction, F_c is sectional force parallel to chord from camber of the airfoil, F_f is sectional force parallel to chord from viscous effects, s is the number of strips and γ is the sectional flap angle.

These aerodynamic forces along with the other body forces are then used with fundamental dynamics equations to determine the motion of BREEZE. The pitching motion of BREEZE can be determined using the following fundamental equations:

$$\theta_n = \theta_{n-1} + (\omega_n * dt) + \alpha_n * dt^2 \quad (10)$$

$$\omega_n = \omega_{n-1} + (\alpha_n * dt) \quad (11)$$

$$\alpha_n = Net\ Torque / I_{yy} \quad (12)$$

Where n is iteration number, θ is vehicle pitch, ω is angular velocity, α is angular acceleration, dt is the time step, and I_{yy} is the moment of inertia of BREEZE about the pitching axis.

Likewise, the same iterative calculation can be applied to find the translation of BREEZE in the X (horizontal) and Z (vertical) directions based on their respective forces. Equations below shown with respect to the X-direction and the Z-direction:

$$x_n = x_{n-1} + (V_{x,n} * dt) + a_{x,n} * dt^2 \quad (13)$$

$$V_{x,n} = V_{x,n-1} + (a_{x,n} * dt) \quad (14)$$

$$a_{x,n} = F_x / m \quad (15)$$

$$z_n = z_{n-1} + (V_{z,n} * dt) + a_{z,n} * dt^2 \quad (16)$$

$$V_{z,n} = V_{z,n-1} + (a_{z,n} * dt) \quad (17)$$

$$a_{z,n} = F_z / m \quad (18)$$

Where, x is forward BREEZE displacement (m), z is vertical BREEZE displacement (m), V is velocity (m/s), a is acceleration (m/s²), dt is the time step (s), F_x and F_z is the sum of the forces in the X and Z directions, and m is the mass of BREEZE (kg).

5.2. Baseline Results

Initially, baseline (non-optimized) parameters were selected for simulating a 12 m and a 36 m BREEZEs' stability and flight dynamics. These are tabulated below in Table 6:

Table 6: BREEZE initial parameters for flight dynamics analysis

Parameter	36 Meter BREEZE	12 Meter BREEZE
Half-wingspan	18.4 m	6 m
Chord	15.2 m	4 m
Max Flap Angle at Wing Tip	30 degrees	30 degrees
Frequency	.235 Hz	.64 Hz
Max Twist at Wing Tip	45 Degrees	45 Degrees
Mass	273.8 kg	10.1 kg
Scientific Payload	54 kg	2.4 kg

The simulation was run for both the twelve-meter (1/3 scale) and thirty-six-meter wingspan (full scale) BREEZE. Both the 12 and 36 m versions showed stable flight. As seen on Fig. 22, 1/3 scale and full-scale BREEZE exhibit an oscillation between a maximum pitch angle of roughly 0.35 degrees and 0.2 degrees, respectively. This suggests that BREEZE is highly stable even with the unsteady aerodynamic forces caused by flapping and could easily correct for deviations through controlling its kinematics using a deep reinforcement learning flight controller. This could be achieved through an asymmetric wing twist or asymmetric wing velocity on the up and downstroke.

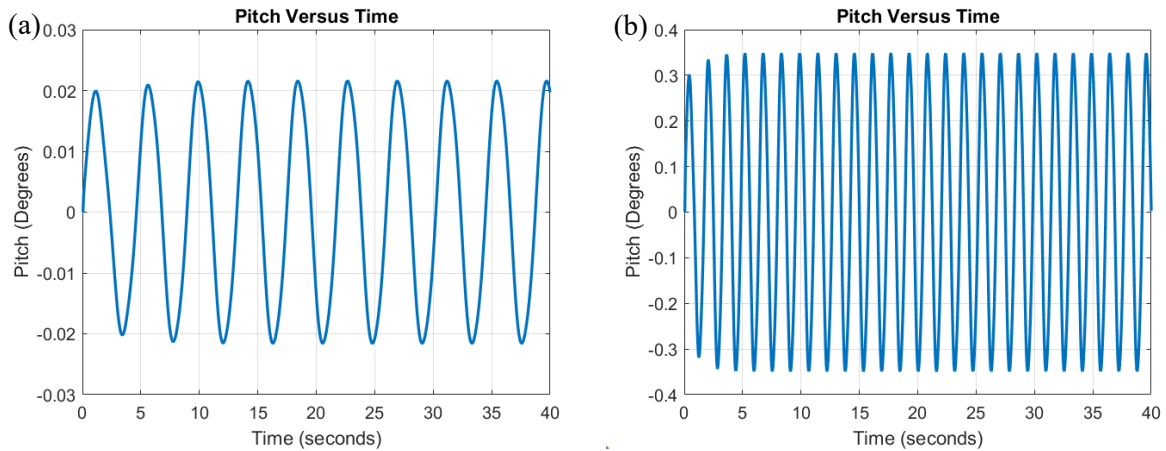


Figure 22: (a) Full scale BREEZE pitch angle over time, (b) 1/3 scale BREEZE pitch angle over time.

BREEZE can achieve this level of stability thanks to its massive moment of inertia (calculated for BREEZE internally in CAD), an inherent attribute of inflatable structures due to the majority of weight being distributed along the outer shell of the structure; this trait is magnified in BREEZE’s case because of its scale reaching a wingspan of roughly 36 m.

Furthermore, the scientific payload is located small distance beneath the center of mass of BREEZE. This also increases BREEZE’s stability. When the vehicle pitches back, the payload will rotate to a position yielding a downwards moment on BREEZE, helping to moderate the pitching of the vehicle during flight by acting as a self-righting feature akin to a ballast on a ship.

BREEZE shows in the simulation an ability to reach, and maintain, a semi-steady-state velocity forwards of ~ 5 m/s. Depicted in Fig. 23, the horizontal velocity can be seen leveling out for both models of BREEZE in minimal amounts of cycles, taking 5 seconds from initiating flapping for 1/3 scale and 12 s for full scale BREEZE to arrive at a steady-state velocity. The 1/3 scale version will have to have a cycle frequency roughly three times faster to achieve the same speed.

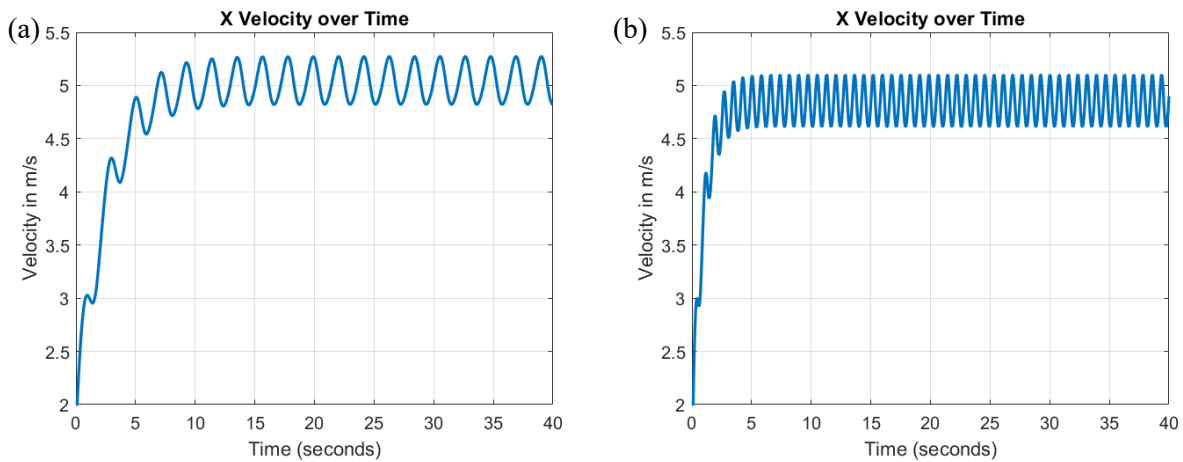


Figure 23: (a) Full scale BREEZE forward velocity over time, (b) 1/3 scale BREEZE forward velocity over time

In addition to examining pitching and forward motion of BREEZE, vertical translation was plotted in Fig. 24. Full scale BREEZE oscillates vertically in a cyclic manner at the same frequency it flaps and with an amplitude of ± 0.9 m. The 1/3 scale BREEZE also oscillates vertically in a cyclic manner at the same frequency it flaps, but with an amplitude of ± 0.3 m. There is no significant net vertical translation of BREEZE over time.

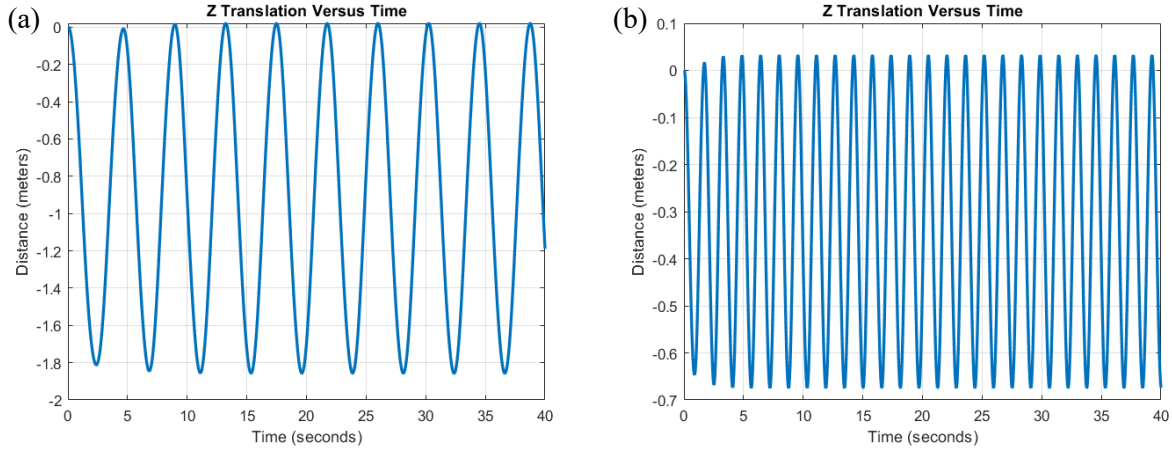


Figure 24: (a) Full scale BREEZE vertical translation over time, (b) 1/3 scale BREEZE vertical translation over time

In addition to vehicle dynamics, the Matlab code allows for rudimentary calculation of power. This is important as it allows endurance and mass estimates presented later in the paper. By multiplying the relative vertical wing velocity and lift of each wing strip and summing the contributions of each strip, power required for propulsion at the achieved flight speed could be determined.

$$P = 2 * \sum_1^s dL * (d\dot{z}) \quad (19)$$

Where P is iteration power (Watts), s is number of sections, dL is sectional lift, and $d\dot{z}$ is wing velocity in the Z-direction. In order to calculate total power. Each section is summed and then multiplied by two to account for both wings. For the full-scale BREEZE, the average power required for flapping propulsion is 1270 W and for 1/3 scale only 103 W for the baseline parameters of each model (Fig. 25).

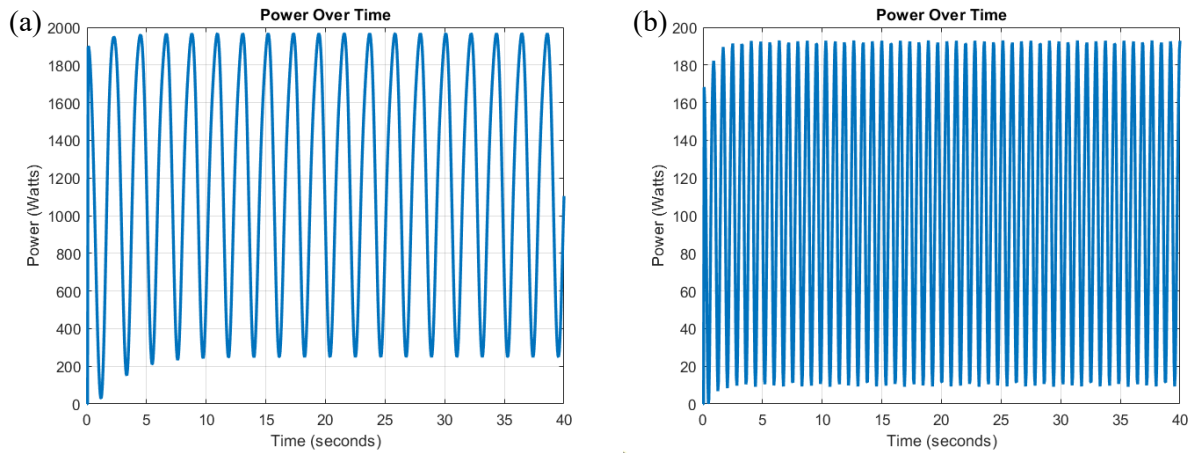


Figure 25: (a) Full scale BREEZE power over time, (b) 1/3 scale BREEZE power over time

5.3. Parametric Study Results

The relationships of BREEZE's fundamental parameters can be observed by incrementally changing parameters such as flapping amplitude or frequency, while keeping other parameters at pre-defined baseline constants, and examining the resulting effects on power, steady-state velocity, pitch, and vertical translation. Due to pitch angle and vertical translation oscillating with averages close to zero, RMS values were utilized rather than average values, and marked accordingly on figures. Power and velocity are averaged values per amplitude or frequency increment. Both full scale and 1/3 scale BREEZE were assessed in this parametric study, with all parameters displaying similar relationships upon scaling down from full to 1/3 scale.

Increasing max amplitude angle unsurprisingly increases both power required and steady state velocity (Fig. 26). Power appears to increase at a quadratic rate, while velocity increases at a more linear rate. This relationship remains almost identical between both full and 1/3 scale BREEZE.

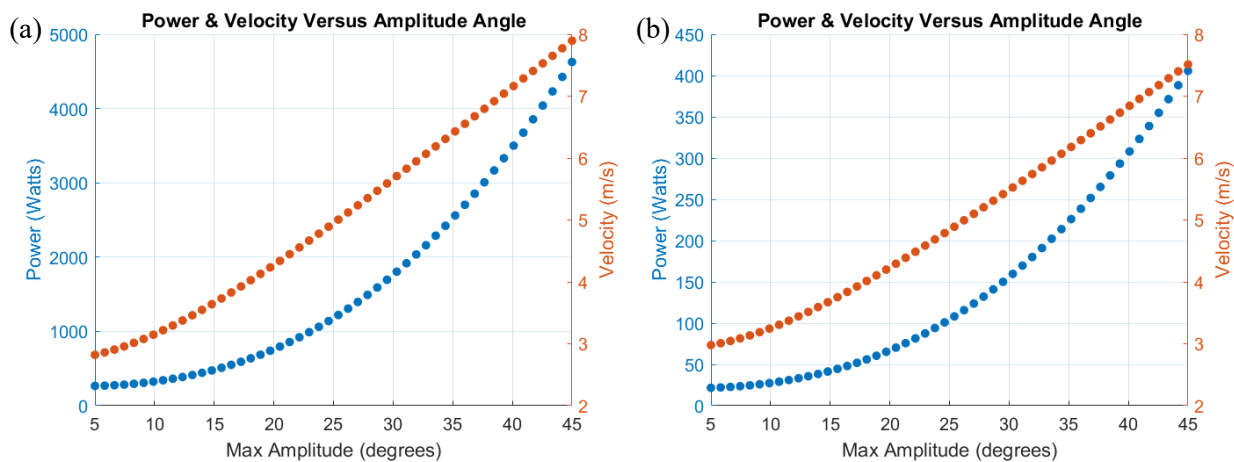


Figure 26: (a) Full scale BREEZE average power and velocity as a function of flap amplitude, (b) 1/3 scale BREEZE average power and velocity as a function of flap amplitude

As for max amplitude angle affecting pitch and vertical translation, there is a more complex relationship found. Surprisingly, there seems to be an optimal angle for minimizing vertical translation and pitching. Based on the simulation, full-scale BREEZE reaches a minimum of pitching at a max flapping angle of 15 degrees, 1/3 scale BREEZE at 17 degrees (Fig. 27).

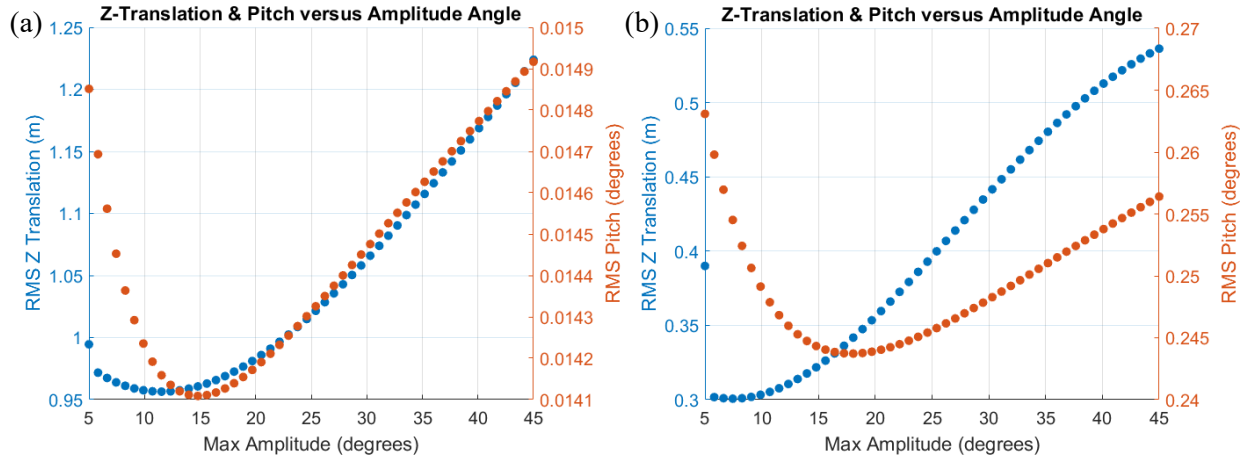


Figure 27: (a) Full scale BREEZE RMS pitch and vertical translation as a function of flap amplitude, (b) 1/3 scale BREEZE RMS pitch and vertical translation as a function of flap amplitude

Alternatively, increasing frequency increases velocity at an almost perfectly linear rate and exponentially increases power required (Fig. 28).

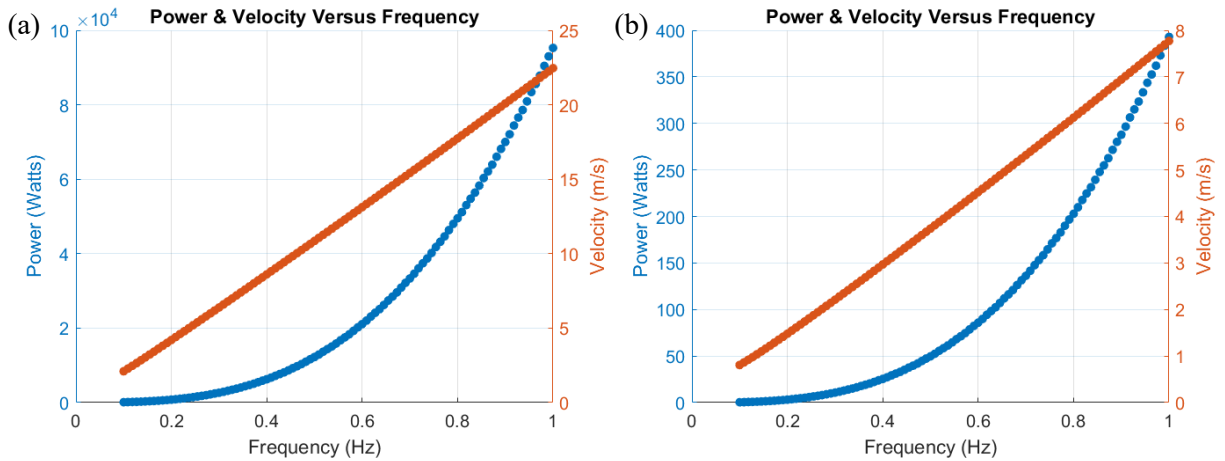


Figure 28: (a) Full scale BREEZE RMS pitch and vertical translation as a function of flap frequency, (b) 1/3 scale BREEZE RMS pitch and vertical translation as a function of flap frequency

Similarly, increasing frequency increases RMS pitch (Fig. 29) at a close to linear rate. The relationship between translation and RMS vertical translation is more complicated, as increasing frequency correlates to an unstable, increasing change in RMS vertical translation. Realistically, BREEZE’s flap frequency would be limited due to the inertial effects of flapping that are not yet considered. Also, BREEZE would be limited in its maximum flap amplitude and wing twist due to bending resistance of the inflatable structure. These effects will be examined more in future studies.

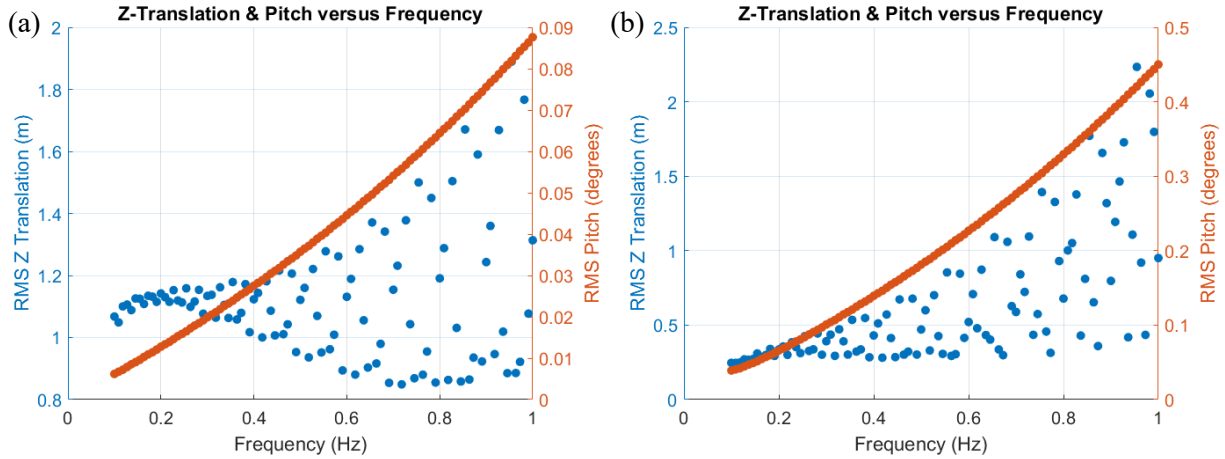


Figure 29: (a) Full scale BREEZE RMS pitch and vertical translation as a function of flap frequency, (b) 1/3 scale BREEZE RMS pitch and vertical translation as a function of flap frequency

6. Structure Analysis and Mass Estimates

6.1. Finite Element Model

In order to determine the structural feasibility of BREEZE for during static loading, a finite element analysis was conducted using Hyperworks. The unique geometry of the inflatable BREEZE wing consists of an airfoil cross section profile with evenly spaced T-shaped ribs through its wingspan (Fig. 30). From the flyer’s symmetry, only one-half section was implicitly analyzed through Optistruct. Since the overall thickness of the membrane and ribs were thin, shell elements were assumed to reduce the computational cost. Through Hypermesh, a first-order, ~50k refined quad-element mesh with a uniform aspect ratio was generated for the membrane and T-shaped ribs.

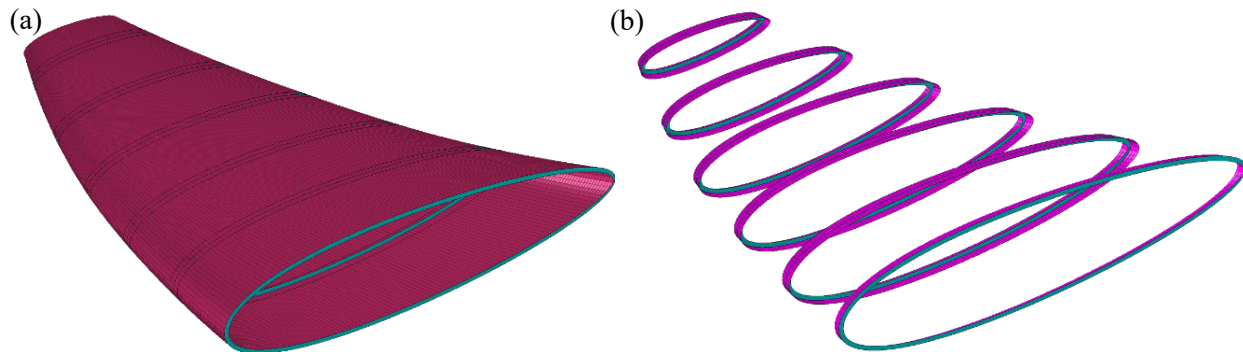


Figure 30: Mesh generation: (a) membrane mesh, (b) rib mesh

6.2. Structural Parametric Studies

Two models were developed, one for a large-scale and another for a small-scale flyer, to compare the optimal number of ribs for reducing high stress concentrations. The major benefit of a large-scale flyer versus a small-scale flyer is the increased payload capacity. From the other perspective, numerous small-scale flyers increase the redundancy of functions and technical equipment thus improving the mission success rate.

Due to the advantageous material properties of composites, kevlar 49 and carbon fiber were applied to the membrane and ribs, respectively. For initial simulations, the materials were treated as linear isotropic using MAT1. To replicate the flyer within Venus' atmosphere, the membrane sustains a uniform outward pressure simulating the overpressure of 2 kPa caused by the lifting gas. Venusian acceleration due to gravity was applied throughout all components of the flyer. For the multiple analyses, the membrane thickness was assumed to be 0.125 mm. The contact between the membrane and ribs were merged nodes. Under the assumption of rigid ribs, the optimal number of ribs for maximum mass efficiency was established through a linear static analysis.

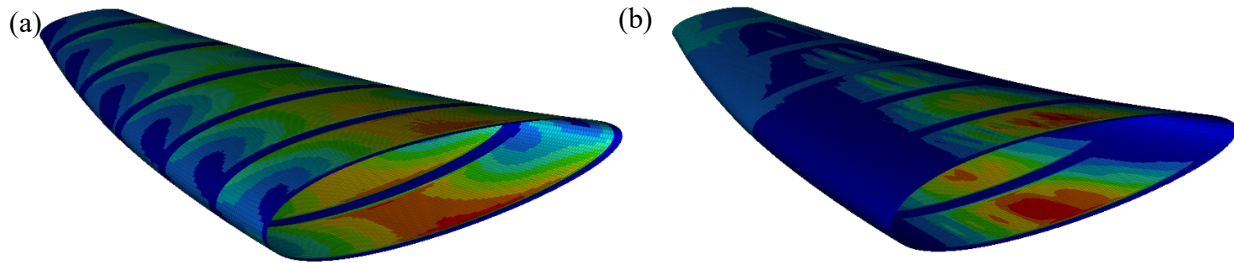


Figure 31: Analysis on an 11-rib flyer (a) stress distribution (b) displacement

Figure 31 shows the stress distribution and displacement on a half-section of an 11-rib large-scale flyer. The maximum calculated stress distribution and displacement appears near the mid-chord of the flyer. Similar results are shown under the same loading conditions and constraints for the small-scale flyer. Figure 32 presents the relation between the maximum stress or displacement versus the number of ribs. From this investigation, an exponential curve was generated based on a 3, 4, 5, 8, 9, 11, and 17 rib system. As seen from the plot, diminishing returns seem to appear after 11-ribs. For this system, the calculated stress was 0.06897 GPa and displacement was 0.02295 m. These initial results are anticipated when BREEZE is sustaining its altitude at 50 or 60 km and not changing altitude through morphing.

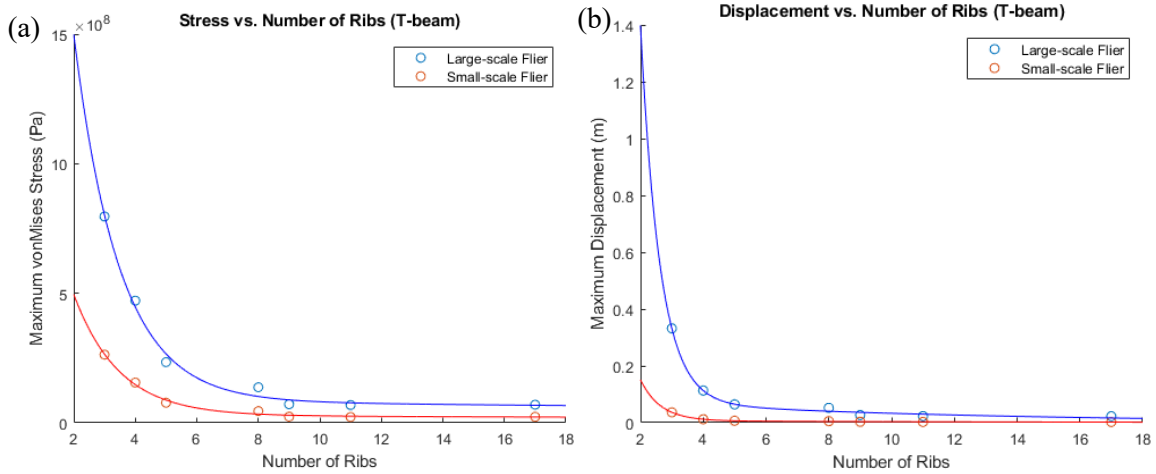


Figure 32: Number of ribs optimization for multiple flyers: (a) stress vs. number of ribs, (b) displacement vs. number of ribs

In addition to optimizing the number of ribs, a series of simulations on different rib geometries were run to minimize stress and displacement while maintaining adequately low stress and deformations in each rib. In these simulations the ribs were no longer assumed to be rigid, and instead a symmetry constraint at the center rib was applied, thus allowing the ribs to deform due to overpressure.

Figure 33 shows the mass versus the maximum stress and displacement when varying the flange lengths, flange thicknesses, and web thicknesses on a large-scale flyer. As one variable changes, the rest are kept constant. The flange and web thicknesses were assumed to be 0.003m, the web length was .140m and the flange length was 0.122m. As seen from the plots, increasing the thickness of the web decreases the maximum stress and displacement at a higher rate compared to changing the other variables. For the length of the flange, it would be best to minimize it since it appears to have the lowest impact on max stress. From these initial simulations, reducing flange and web thickness before modifying flange length would increase the mass efficiency of the flyer.

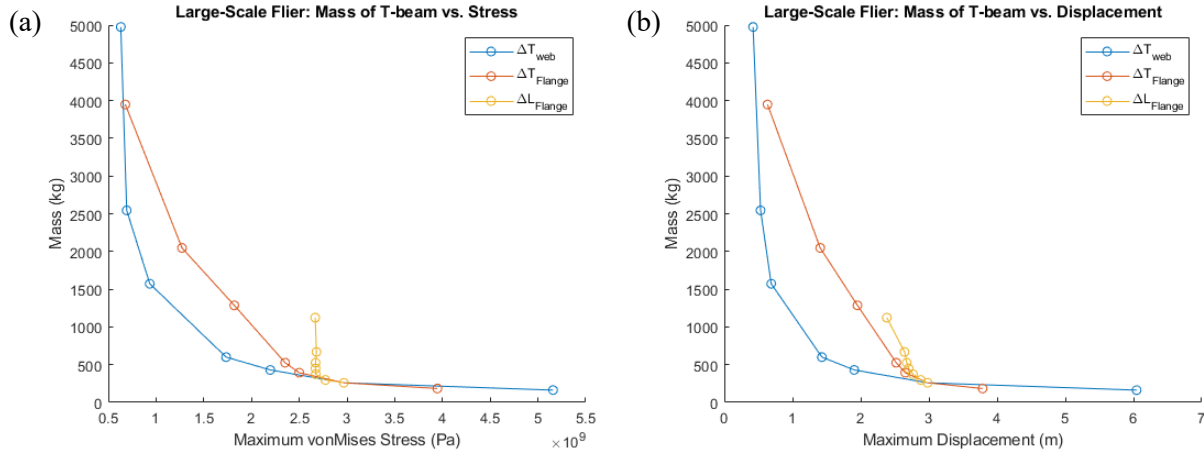


Figure 33: Initial rib cross-section optimization on a large-scale flyer: (a) mass vs. stress, (b) mass vs. displacement

From these initial mass optimizations, vertical stiffeners were added to each section of the ribs. The same loading conditions and constraints remained from the previous models. Figure 34 illustrates the stress distribution across the membrane and ribs. The stress distribution for the membrane was relatively similar to the rigid rib assumption. As for the stress distribution along the ribs, the maximum stresses appear around the contact point of the vertical stiffeners and web of the T-shaped rib.

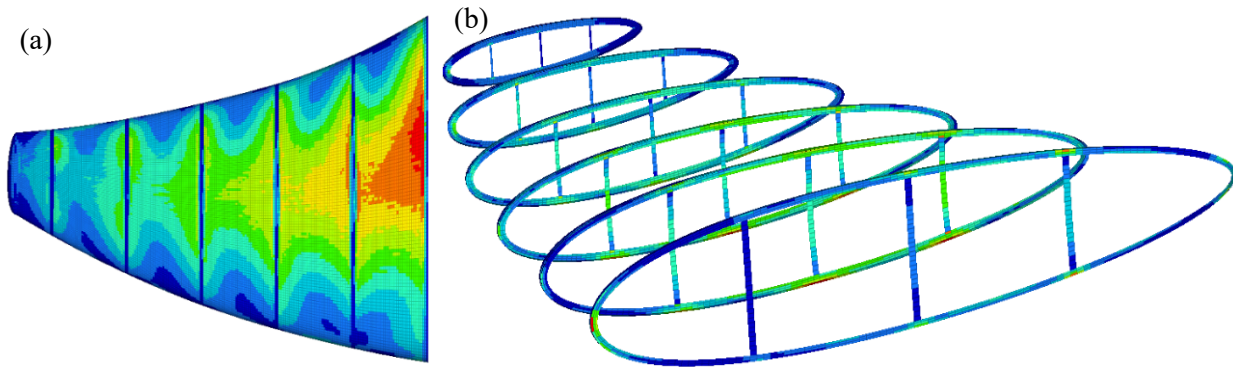


Figure 34: von Mises stresses. (a) membrane stress distribution (b) rib stress distribution

6.3. Structural Scaling Effects

Using the partially optimized geometry from previous simulations, four scaled versions of BREEZE were created for comparison. This scaling study was conducted to determine the possibility of using multiple different scaled flyers for a mission. All geometric dimensions including thicknesses were proportionally scaled between cases, and the same amount of internal over pressure being applied at every scale. Table 7 was generated to present the sizing and mass parameters for multiple BREEZE flyers. In Table 7 total mass was set as the mass required for BREEZE to achieve neutral buoyancy at 60 km. Since BREEZE scales proportionally, the structural mass for the flyers selected accounted for 45% of the

maximum allowable mass for neutral buoyancy. Helium contributes to approximately 9% more mass, while hydrogen adds roughly around 4.2% to this average. Overall, with the current structural design (which could still be further optimized) BREEZE has more than 45% of its mass available for payload, actuators, batteries, and solar panels.

Table 7: Sizing parameters of multiple BREEZE flyers

Parameter	1:1 Scale	7:9 scale	5:9 scale	1:3 scale	Units
Wingspan	36.80	28.48	20.36	12.20	m
Centerline Chord Length	15.20	11.66	8.32	4.97	m
Total Volume	569.78	267.46	97.06	20.76	m ³
Total Mass	276.01	129.56	47.02	10.02	kg
Structural Mass	124.60	57.76	21.10	4.54	kg
Helium Mass	25.11	11.78	4.28	.915	kg
Hydrogen Mass	12.64	5.94	2.15	.461	kg
BREEZE Overpressure	.20	.20	.20	.20	kPa
60-50 km required volume change	70.6	70.6	70.6	70.6	%

The 1:1 scale flyer experiences maximum rib and membrane stresses of 0.5857 GPa and 0.2862 GPa, respectively. As seen from Table 8, the stresses are close to identical across different scales. From the resulting relationship, multiple sized flyers can be produced with the instrumentation and equipment distributed among them being equivalent to the amount of equipment carried by a larger flyer of equal mass. This proves to be advantageous since flyers can be proportionally sized for the desired mission or BREEZE can be used as a secondary payload on another mission.

Table 8: FEA max stress of multiple BREEZE flyers

Parameter	1:1 Scale	7:9 scale	5:9 scale	1:3 scale	Units
Maximum Rib Stress	585.7	584.6	583.5	582.5	MPa
Maximum Membrane Stress	286.2	288.3	286.2	287.3	MPa

6.4. Mass Breakdown of BREEZE

In addition to the structure, workable mass is partitioned into categories of solar panels, lifting mass, batteries, tensioning actuators, and scientific payload. Wing actuation through tensioning is intended to be driven using a number of high-torque, low-RPM motors driving twisted string actuators. Considering recent advances in motor technology, power densities as high as 7.1 kW/kg can be achieved [25]. If BREEZE's actuation mechanisms are allotted 2 kg of mass, it is estimated they will have an estimated output of 14.2 kW, which is more than 7 times the power required to resist 5 m/s meridional winds.

Based on the total power requirements for the tensioning twisted string actuators, the required number of solar panels are determined. The selected solar panels are flexible, with an areal density of 0.25 kg/m² and efficiency of 20% [26]. Using the results of an investigation on triple-junction solar cells as a baseline, conducted by Landis and Haag [27], the expected solar power density, including intensity and temperature corrections as a function of altitude will be 383.5 W/m² at 60 km, and 175 W/m² at 50 km. By using 44 m² of solar panels with a total mass of 11 kg, enough power is collected from these panels to continuously drive the tensioning actuators, power onboard equipment, and recharge the BREEZE's batteries.

Batteries will be required to power the scientific payload during the Venus night, which is at most approximately three Earth days considering the speed of the zonal winds at the target altitudes. The power requirements of the scientific payload are based on the Venus Flagship DRM balloon payload, which required 50 W for a 20 kg payload [28]. With the 50 kg of scientific payload to be allocated for the proposed mission, a power draw estimate of 125 W was made, which becomes 9 kW-hr for the scientific instruments to operate continuously through the Venus night. Additionally, some extra power is desired to allow BREEZE to maneuver if an unexpected situation arises during the night when no power can be collected from the solar panels. State-of-the-art batteries can achieve a power density of 500 W-hr/kg for lithium based systems, which can safely operate within the range of temperatures expected for the target altitude range [29]. 50 kg allotted for battery mass would allow for the storage and utilization of up to 25 kW-hr. In addition to providing continuous power to the scientific instruments, the leftover power allows BREEZE to flap for up to an estimated 12 hours at 5 m/s. This is comparable to the amount of drift that will be experienced in the three Earth day period on the night-side of the planet. Even if the flapping is never used and the craft drifts with the meridional winds for the entire Venusian night, the craft can easily make up the distance in less than a single Earth day.

The additional non-allocated mass of 13.3 kg if helium is used as the lifting gas, and 25.8 kg if hydrogen is used for inflation, will be available to be used for energy storage or for additional scientific payload. Enhancing energy storage would increase the navigational capabilities of BREEZE by extending the

longevity of the powered flight on Venus' dark side, while additional payload would allow BREEZE to complete a number of secondary science objectives.

7. Broader Impact

Due to the BREEZE system's wide range of functionality its applications extend well beyond Venus. The kinematics developed in this study can be non-dimensionalized and applied to the exploration of other high density celestial bodies or even the unexplored regions of Earth's oceans. An oscillatory autonomous underwater vehicle (AUV) spinoff of BREEZE would be agile, efficient, and cause minimal disturbance to its surroundings. Furthermore, due to its endurance, BREEZE could be used in Earth's atmosphere as a telecommunications relay similar to Facebook's Aquila Drone, and Google's Titan and Loon systems, currently under development, although the hybrid system that BREEZE employs makes it even more versatile than the former systems.

8. Future work

Detailed EDI analysis could be conducted using NASA's Program to Optimize Simulated Trajectories II (POST2) coupled with Adams, a multibody dynamics simulation tool. Detailed EDI analysis will help develop design specifications for the entry vehicle and, consequently, a total mission mass estimate.

Continued CFD analysis could include modeling more accurate flow behavior surrounding BREEZE. The wind near the base of the upper cloud layer and the lower cloud layer is uniform, similar to Earth's atmosphere. However, under extreme wind conditions, BREEZE might experience gust. Turbulence modeling combined with gust input will offer an accurate strategy to capture the details of BREEZE's flight in Venus. Performing CFD simulations on BREEZE flyers of different scales would increase understanding of the effect of scaling on the aerodynamics of the vehicle, which will help determine different applications of the system. Lastly, a parametric study of fluid parameters such as density, temperature, and viscosity could be performed and become the groundwork to assess the adaptability of BREEZE to other celestial environments such as Earth's atmosphere, ocean, or Titan's atmosphere.

Further virtual free flight analysis could be conducted. While the current analysis gives an initial understanding of the stability and flight dynamics of BREEZE, inertial effects of the wing, as well as a higher fidelity aerodynamics model, could be incorporated. This would increase accuracy and allow for the training of a robust flight control system based on an artificial neural network and deep reinforcement learning.

To generate more accurate FEA results, Venus' environmental properties, such as thermal gradients and dynamic pressure forces caused by BREEZE's bioinspired propulsion, could be implemented into the simulations. Also, the morphing of the wing could be implemented by applying tensile forces throughout the wing to mimic the tensioning cables. Lastly, a fabric material model could be implemented. The linear elastic model currently used is adequate for simple overpressure simulations, but a fabric model would allow for large deformations caused by wing morphing to be accurately modeled.

Almost all analysis on BREEZE thus far has been done using analytical or computational methods. In order to push the concept to a higher technology readiness level, laboratory testing on small scale prototypes should be performed. Planned testing includes motion capture of a BREEZE prototype to test actuation methods, compression testing to test buoyancy control, and wind tunnel testing to assess BREEZE's propulsion capabilities as well as validate aerodynamic models and CFD simulations.

9. Conclusion

BREEZE is a bioinspired inflatable flyer that combines the strengths of a number of proposed Venus flyers. BREEZE's hybrid characteristics allow for controlled navigation within Venus' atmosphere as well as continuous operation on the less explored night side. BREEZE will conduct dispersed sample collection for atmospheric and geographic studies on Venus. This report discusses NIAC phase I work, which includes several different sub-studies. First was designing a conceptual mission to Venus that would utilize BREEZE. Second, was applying CFD to determine the thrust capabilities of BREEZE's bioinspired propulsion. The third was using a MATLAB environment to analyze the flight dynamics and stability of BREEZE. A fourth was using finite element analysis to design and optimize BREEZE's inflatable wing. Last was conducting mass estimates based on power requirements and structural analysis.

Key results from these sub-studies are as follows. BREEZE's bioinspired propulsion can generate net thrust at speeds of 5 m/s, allowing it to make headway against Venus' meridional winds. BREEZE's relative angle of attack, flapping amplitude, and Strouhal number could be tuned during flight to adjust thrust production. BREEZE is stable during flight thanks to its large moment of inertia and its buoyant structure paired with a low center of gravity. From a structural standpoint, BREEZE scales ideally between different size flyers. This increases its versatility and makes it suitable as a secondary payload or in a small multi-flyer mission. Initial estimates indicate that BREEZE would have 18% of its mass or more available for scientific instrumentation. While there are still many unknowns associated with BREEZE, which is expected for a new high-risk high-reward concept, initial results are promising, and further study could ultimately result in a comprehensive yet cost-effective mission to Venus.

10. Acknowledgements

The award of the NASA Innovative Advanced Concepts (NIAC) Program Phase I grant that made the present exciting research pursuit possible is highly acknowledged and appreciated. The authors would like to personally thank each and every member of the NIAC Executive and Program Teams, NIAC Scientific Advisory Board, and the NASA Space Technology Mission Directorate that created and supported such an important scholarly and cultural undertaking.

The authors would further like to thank NASA Langley Research Center for their dedicated support and helpful insights.

Additionally, the authors wish to express their gratitude for the time and efforts that Suraj Megharaja, Pradeep Vaghela, Peitro Aiazzone, Nicholas Deitrich, and the other members of *CR*ashworthiness for *Aerospace Structures* and *Hybrids Laboratory (CRASH Lab)* as part of the Department of Mechanical and Aerospace Engineering of University at Buffalo, The State University of New York afforded in assisting with deriving the technical approach, strategy and analysis.

11. References

- [1] Preston, R.A., et al., "Determination of Venus winds by ground-based radio tracking of the VEGA balloons." *Science*, 231.4744, 1986: 1414-1416.
- [2] Shao-bo, Y., Qiu, J., and Han, X.U., "Kinematics modeling and experiments of pectoral oscillation propulsion robotic fish." *Journal of Bionic Engineering*, 6.2, 2009: 174-179.
- [3] Zhou, C., and Low, K.H., "Design and locomotion control of a biomimetic underwater vehicle with fin propulsion," *IEEE/ASME Transactions on Mechatronics*, 17.1, 2012: 25-35.
- [4] Feaster, J., Battaglia, F., & Bayandor, J., "A Computational Study on the Influence of Insect Wing Geometry on Bee Flight Mechanics." *Biology Open*, 2017.
- [5] Dadashi, S., Feaster, J., Bayandor, J., Battaglia, F., & Kurdila, A. J., "Identification and adaptive control of history dependent unsteady aerodynamics for a flapping insect wing." *Nonlinear Dynamics*, 85.3, 2016: 1405–1421
- [6] Gater, B., Feaster, J., and Bayandor, J. "Dynamics and Propulsive Efficiency of Bio-inspired Undulatory Marine Locomotion," *FEDSM2016-7742*, Washington, D.C., 2016.
- [7] Sharp, N.M.W., Hagen-Gates, V., Hemingway, E., Syme, M., Via, J., Feaster, J., Bayandor, J., Jung, S., Battaglia, F., and Kurdila, A., "Computational Analysis of Undulatory Batoid Motion for Underwater Robotic Propulsion," *FEDSM2014-22077*, Chicago, IL, 2014.

- [8] Feaster, J., Matta, A., Battaglia, F., Kurdila, A., Müller, R., and Bayandor, J., “A Methodology for the Kinematic and Unsteady Dynamics Analysis of Bat Flight,” *FEDSM2014-22118*, Chicago, IL, 2014.
- [9] Matta, A., and Bayandor, J., “Low Order Modeling of the Unsteady and 3D Effects of Continuous Wake Flapping Flight,” *ICAS 2016-0651*, Daejeon, South Korea, 2016
- [10] Matta, A., and Bayandor, J., “An Analytical Study on the Effect of Active Wing Folding and Twist on the Aerodynamic Performance and Energy Consumption of a Bio-inspired Ornithopter,” *FEDSM2016-7741*, Washington, D.C., 2016.
- [11] Harrington, A., Kroninger, C., “Characterization of Small DC Brushed and Brushless Motors,” *ARL-TR-6389*, Army Research Laboratory, 2013.
- [12] Summers, A., Picturing Science, <http://www.picturingscience.com/clearedstained/>
- [13] Fimmel, R., Colin, L., and Burgess, E., “PioneerVenus,” *NASA SP-461*, 1983.
- [14] Hall, J.L., et al., “Prototype design and testing of a Venus long duration, high altitude balloon.” *Advances in Space Research*, 42.10, 2008: 1648-1655.
- [15] Justus, C.G., and Braun, R.D., “Atmospheric Environments for Entry, Descent and Landing (EDL),” 2007.
- [16] Bugga, R., “Venus Interior Probe Using In-situ Power and Propulsion (VIP-INSPR),” 2016
- [17] Sánchez-Lavega, A., Hueso, R., Piccioni, G., Drossart, P., Peralta, J., Pérez-Hoyos, S., Wilson, C.F., Taylor, F.W., Baines, K.H., Luz, D., Erard, S., and Lebonnois, S., “Variable winds on Venus mapped in three dimensions.” *Geophysical Research Letters*, 35.13, 2008: L13204.
- [18] Limaye, S., Mogul, R., Smith, D., Ansari, A., Słowik, G., and Vaishampayan, P., “Venus' Spectral Signatures and the Potential for Life in the Clouds,” *Astrobiology*, 18.9, 2018: 1181-1198.
- [19] Schulze-Makuch, D., Grinspoon, D., Abbas, O., Irwin, L., and Bullock, M., “A Sulfur-Based Survival Strategy for Putative Phototrophic Life in the Venusian Atmosphere,” *Astrobiology*, 4.1, 2014: 11-18.
- [20] ANSYS Incorporated, *Fluent 19.0 User's Guide*, 2019
- [21] Fish, F. E., Schreiber, C. M., Moored, K. W., Liu, G., Dong, H., and Bart-Smith, H., “Hydrodynamic performance of aquatic flapping: efficiency of underwater flight in the manta.” *Aerospace*, 3.3, 2016: 20.
- [22] Vandenberghe, N., Zhang, J., & Childress, S., “Symmetry breaking leads to forward flapping flight.” *Journal of Fluid Mechanics*, 506, 2004: 147–155.

- [23] Eloy, C., "Optimal Strouhal number for swimming animals." *Journal of Fluids and Structures*, 30(1), 2012: 205–218
- [24] Kim, D., Lee, J., and Han, J., "Improved Aerodynamic Model for Efficient Analysis of Flapping-Wing Flight." *AIAA Journal*, 49.4, 2011: 868-872
- [25] Rogers, S.A., "Annual progress report for the advanced power electronics and electric machinery program," *2005 Annual Progress Report, Vehicle Technologies Program, US DOE*, Washington, DC, 2005.
- [26] Johnson, C.L., et al., *Lightweight Inflatable Solar Array: Providing a Flexible, Efficient Solution to Space Power Systems for Small Spacecraft*, 2014.
- [27] Landis, G.A., Haag, E., "Analysis of solar cell efficiency for Venus atmosphere and surface missions," *11th International Energy Conversion Engineering Conference*, San Jose, CA, 2013.
- [28] Bullock, M.A., Senske, D.A., Balint, T.S., Benz, A., Campbell, B.A., Chassefière, E., et al., *Venus Flagship Mission Study: Report of the Venus Science and Technology Definition Team*, JPL, 2009.
- [29] Davis, J.M., et al., "An overview of power capability requirements for exploration missions," *NASA-TM-2005-213600*, NASA Glenn Research Center, 2005.